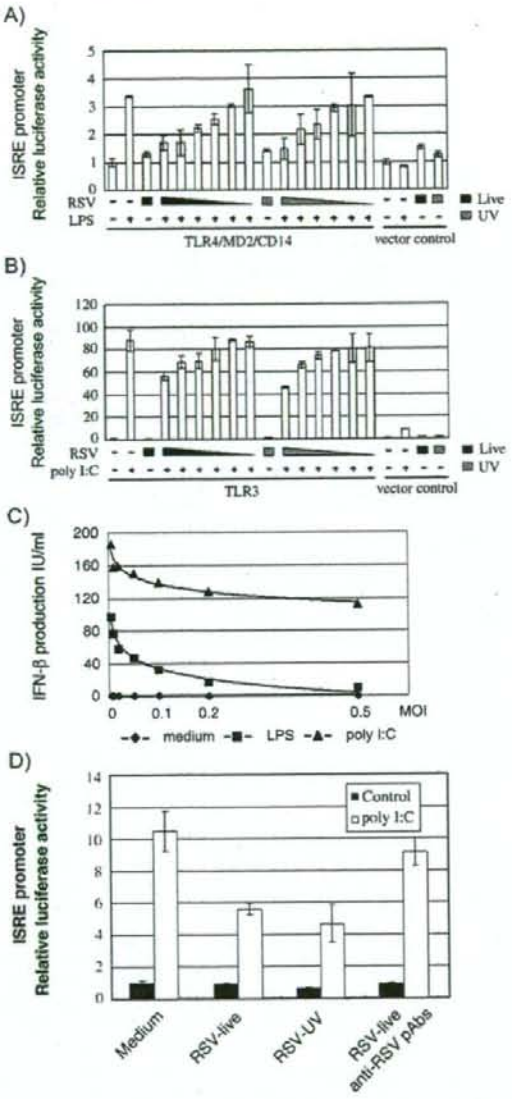

Fig. 4. RSV inhibits TLR-dependent IFN-β induction. (Panels A and B) RSV inhibits reporter activation by ISRE promoter. HEK293 cells were transfected with pISRE-Luc and phRL-TK plasmid, together with the pEFBos TLR4 plasmid sets (TLR4, MD-2 and CD14) (13) or TLR3 plasmid. Twenty-four hours later, cells were washed and treated with various doses of RSV (MOI = 0.5, 0.2, 0.1, 0.05, 0.02 and 0.01) in the presence or absence of LPS (A) or polyI:C (B). Six hours after incubation, cell lysates were subjected to the assay for the dual reporters (13). Fold induction against the medium control is indicated. (Panel C) Immature mDCs were treated with UV-irradiated RSV (MOI indicated) together with LPS or polyI:C. Twenty-four hours later, culture supernatants were collected and the levels of IFN-β measured by ELISA. (Panel D) RSV-mediated inhibition of ISRE promoter activation is abrogated by the addition of pAbs against RSV. HEK293 cells with TLR3 and ISRE promoter were treated with polyI:C (medium) and live (RSV-live) or inactive RSV (RSV-UV) (as in B). Under the conditions where the RSV-mediated inhibition was observed, pAbs against RSV were added to the cells (RSV-live, anti-RSV pAbs). Six hours after incubation, cell lysates were subjected to the assay for the dual reporters.

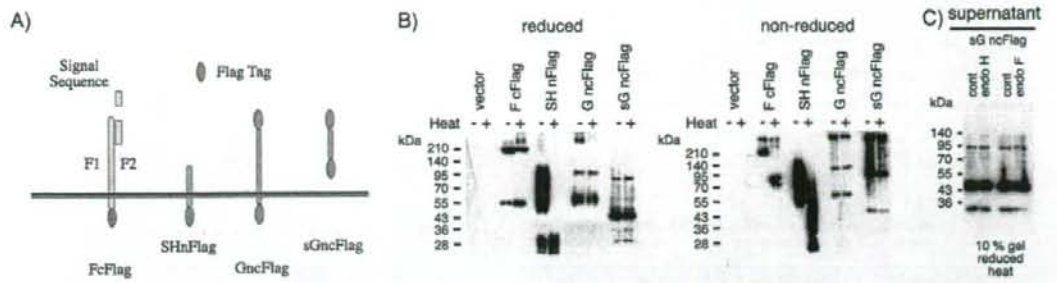

Fig. 5. Detection of the RSV envelope proteins expressed on HEK293 cells. (Panel A) Scheme of the Flag-tagged RSV proteins. Predicted proteins are shown based on the constructs we prepared. F, SH, G and sG are RSV envelope proteins. Flag-labeled (N-terminal, n and/or C-terminal, c) is indicated. Elliptic circles indicate the Flag-tag. FcFlag, C-terminal-flagged F protein; SHnFlag, N-terminal-flagged SH protein; GncFlag, both N- and C-terminal-flagged G protein; sGncFlag, N- and C-terminal-flagged secreted G protein. (Panel B) Immunoblotting analysis of RSV envelope proteins in HEK293 cells. Cells were transfected with the plasmids encoding the RSV envelope proteins tagged with Flag (see A). Twenty-four hours later, cell lysates were immunoprecipitated with anti-Flag antibody and the proteins were resolved on SDS–PAGE (10% gel) under reducing (left panel) or non-reducing conditions (right panel). After protein blotting onto a sheet, blots were probed with anti-Flag pAb. (Panel C) Glycosylation of RSV proteins liberated from HEK cells. The supernatants of the sGncFlag-transfected HEK293 cells in (B) were treated with endoglycosidase H (endo H) or endoglycosidase F (endo F) and analyzed on SDS–PAGE followed by immunoblotting. The conditions of the analyzed samples are shown in the panel.

We found RSV inducing minimal IFN-β through virion–cell attachment (usually taking <4 h p.i.) and then inducing robust IFN-β after cytoplasmic replication (>12 h p.i.). The F protein should be an effector for the RSV-mediated IFN-β induction, but somehow the IFN-β induction tends to be diminished in RSV–host cell interaction. We searched for the factor negatively regulating IFN-β induction in host HEK293 cells using UV-inactive RSV and found that attachment of RSV envelope proteins to host cells causes down-regulation of IFN-β. Finally, the G protein of RSV is the factor for the inhibition of IFN-β promoter activation: even by the stimulation with polyI:C or LPS, bystander inhibition happens by function of the soluble form of the G protein (sG). Addition of the sG protein to the culture of mDCs allows the suppression of polyI:C- or LPS-mediated IFN-β production. Ultimately, here we disclose a novel function of the RSV G protein in the regulation of host cell IFN response.

Using *in vitro* analysis, we found that the RSV F protein-mediated IFN induction (30) is neutralized by the RSV G protein, which selectively modulates the TICAM-1 pathway, i.e. the preferential activation of IRF-3 and the IFN-β promoter in myeloid DCs. The G protein can inhibit both TLR3 and TLR4 to suppress IFN-β induction, supporting the target TICAM-1. Studies using reporter analysis, ELISA with mDCs and gene-silencing analysis of MAVS and TICAM-1 using RNAi (M. Matsumoto and T. Seya, unpublished data) all supported the G protein function in the TICAM-1 pathway.

How the G protein modulates the TICAM-1-mediated IFN-inducing function remains as a tantalizing point in this story. A possible molecular mechanism is that the G protein is produced after replication and a putative receptor for the G protein delivers a negative signal to the TICAM-1 pathway. This G protein receptor may exist in the cytoplasmic compartment or on cell surface and link the TICAM-1 pathway in the cytoplasm. This hypothesis may be related to the fact that a defective recombinant virus lacking the sG protein decreases the virus pathogenicity due to the induction of antiviral immunity (40). In addition, how dsRNA stimulation activates TICAM-1 is getting clear in a molecular level (41). Furthermore, a recent report (42) suggested that the TIR-containing adaptor SARM exhibits a regulatory function toward TICAM-1. Further studies are required to clarify the mode for TICAM-1 inhibition by extrinsic G proteins.

Since IFN-inducible genes are significantly up-regulated in mDCs in response to live RSV after 24 h p.i. (Fig. 2C), the initial trigger of IFN induction by live RSV may be too weak to suppress RSV replication, so that the infected mDCs elicit following replication-mediated response. In fact, importance of 'revving up' activation of IFN-β for amplifiable IFN-α/β response has been proposed in a recent review (43). RIG-I and MDA5 are preferentially responsible for the replication-dependent antiviral event in response to live viruses, which is evident in the airway epithelial cells (6). Since RIG-I and MDA5 are IFN-inducible proteins, an initial trigger of IFN-β also critically causes their induction in virus-attached cells. We surmise the importance of F protein-mediated TLR4 signal in an early response of cells to RSV. Blocking of the F protein function by G proteins may be crucial for silencing the IFN-inducing response and for the virus side facilitating RSV infection. Indeed, immature mDCs secrete TNF-α and mature in a similar manner in response to both live and dead RSV, possibly reflecting minute participation of type I IFN in the RSV-mediated maturation phenotype of mDCs.

The difference in outcome between TLR and RIG-I/MDA5 signaling is an intriguing question. TLR3 senses viral RNA outside the cytoplasm and RIG-I/MDA5 sense it inside the cytoplasm. RIG-I/MDA5 and TLR3 recruit different adaptors, IPS-1 and TICAM-1, respectively. Although TICAM-1 and IPS-1 interact partly with TANK family proteins (10, 44), only the TICAM-1 pathway is reported to elicit potencies to activate CTL and NK cells in mDCs (11, 12). Our premise is that viral RNA replication inside the cytoplasm and extrinsic dsRNA stimulation lead to differential mDC driving. Selective inhibition

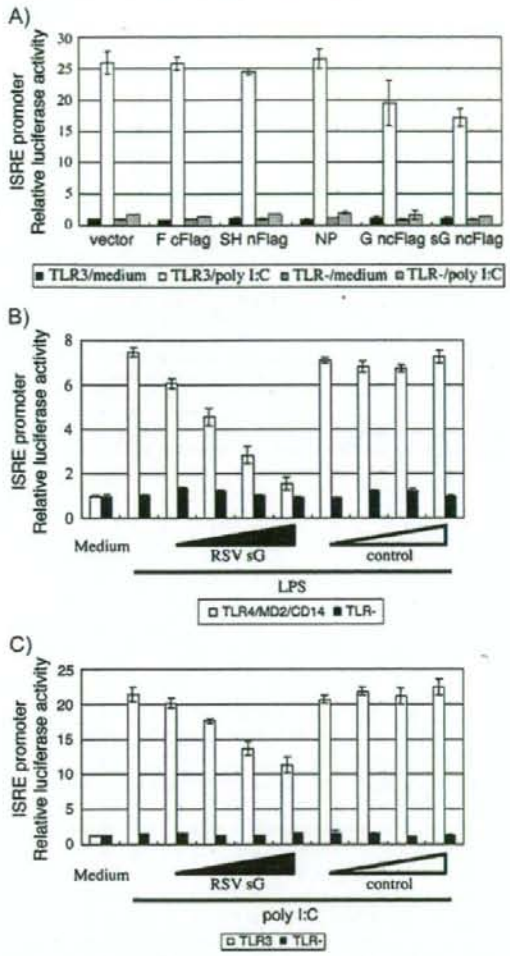

Fig. 6. RSV G protein inhibits activation of the ISRE promoter. (Panel A) RSV G protein inhibits ISRE activation by TLR3. HEK293 cells were transfected simultaneously with pISRE-Luc, phRL-TK, pEFBos TLR3 and indicated plasmids encoding RSV proteins. Twenty-four hours later, cells were incubated with 10 μg ml^{-1} of polyI:C or buffer only. After 6 h, dual-luciferase reporters were assayed as in Fig. 4(A). (Panel B and C) sG protein inhibits ISRE activation by LPS or polyI:C. HEK293 cells expressing TLR4/MD-2/CD14 or TLR3 were prepared and then the ligand stimulation was added to the cells in the medium containing RSV sG. HEK293 cells were transfected with pISRE-Luc, phRL-TK and pEFBos TLR4 expression plasmids or TLR3 plasmid. Twenty-four hours later, cells were stimulated with 100 ng ml^{-1} of LPS (B) or 10 μg ml^{-1} of polyI:C (C) under various doses of RSV sG (1/5, 1/10, 1/20 and 1/40 volumes of medium). The culture supernatant from the empty vector-transfected cells was used as a control. After 6 h incubation, luciferase reporter activity was measured as in Fig. 4(A). The figures are representative results of multiple trials.

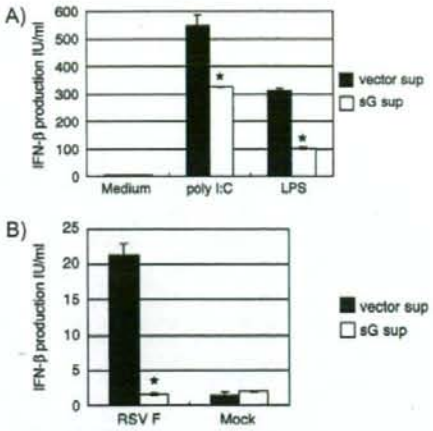

Fig. 7. RSV sG protein inhibits IFN-β production by mDCs stimulated with polyI:C or RSV F protein. (Panel A) sG protein inhibits polyI:C-inducing IFN-β production in human mDCs. mDCs were prepared as in Fig. 1. Cells were stimulated with polyI:C in the presence of the sG protein-containing or control medium. Twenty-four hours later, the supernatants were harvested to measure the IFN-β content. LPS was used as control as in Fig. 2(D). (Panel B) Purified F protein allows mDCs to produce IFN-β, which is inhibited by sG. Immature mDCs were stimulated with the purified F protein (1 μg) in the presence or absence of the sG-containing medium. Twenty hours later, the IFN-β levels released in the supernatant of mDCs were determined by ELISA.

of the TICAM-1 pathway may benefit RSV survival and happen to suppress mDC-derived cellular immune responses. Severe repetitive infection by RSV occurring in children and being referred to insufficient mDC maturation, may be partly due to this extrinsic mDC regulation by RSV proteins.

The question is whether the early IFN induction via RSV-attached host cells is physiologically significant in mDCs. A number of RSV studies have suggested that TLR3 is implicated in the immune response of epithelial cells. IL-8, RANTES, TNF-α and IL-6 are up-regulated secondary to RSV infection (45–47). In addition, IFN-inducible genes, including *TLR3* and *PKR*, are up-regulated (5). These findings were reported before the molecular identity of RIG-I/MDA5 was completed and were based on the assumption that the source of dsRNA was from RSV RNA released from cells undergoing infection-induced apoptosis. It is still unclear whether the virus–cell attachment-mediated TICAM-1 blocking earlier and more significantly participates in initial IFN induction than the intrinsic cytoplasmic IFN-inducing pathway. However, in RSV infection, this G protein-mediated TICAM-1 blocking would be crucial since RSV possesses the TLR4 ligand F protein. The question is whether these findings are adaptable to human patients with RSV infection. Further analysis will be required about what happens in mDCs and acquired immunity once replication-derived viral RNA products are generated in patients' body (8, 9).

Regarding viral aspects, a recent report suggested that the G cysteine-rich region of the RSV sG protein inhibits production of NF-κB-inducible inflammatory cytokines through TLR4 (48). Since MyD88 is not a target of the RSV G

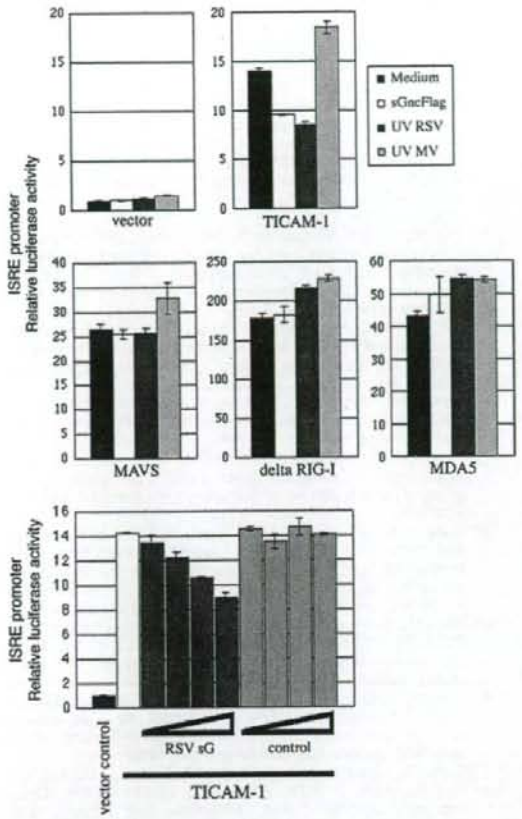

Fig. 8. The sG protein inhibits the TICAM-1 pathway. (Panel A) The sG protein blocks TICAM-1-mediated ISRE promoter activation. HEK293 cells were treated with a control medium or medium containing sG along with control dead RSV or MV and transfected with pISRE-Luc, phRL-TK and the plasmids expressing for the indicated proteins. Six hours later, cells were washed, lysed with lysis buffer and the reporter assay was performed as in Fig. 4(A). (Panel B) The sG protein dose dependently inhibits the TICAM-1 pathway. HEK293 cells were transfected with the TICAM-1 plasmid, and the TICAM-1-mediated ISRE promoter activation was monitored in the presence of variable amounts of the RSV sG-containing medium (1/5, 1/10, 1/20 and 1/40 volumes of medium). The culture supernatant from the empty vector-transfected cells was used as a control.

proteins in NF-κB activation (data not shown), the G protein can distinguish between MyD88 and TICAM-1 as the molecular target. Besides the RSV F protein, many viral envelope proteins are known to act as ligands for TLR2 or TLR4. In general, many viral proteins reportedly inhibit the JAK/STAT pathway and IRF-3 activation. NS3/4A of HCV inactivates IPS-1 and TICAM-1 by proteolysis (49). Vaccinia virus proteins also target TLR adaptor proteins (50). RSV NS1 and NS2 are simultaneously generated with viral RNA in the cytoplasm. These proteins act as inhibitors for IFN-α/β signaling after replication (26, 27). Here, we add to these findings a line of evidence that the RSV G protein is a negative regulator for the TLR3/4-mediated TICAM-1 pathway.

Funding

CREST and Innovation; Japan Science and Technology Corporation; Program of Founding Research Centers for Emerging and Reemerging Infectious Diseases; MEXT; Ministry of Education, Science, and Culture (Specified Project for Advanced Research); Ministry of Health, Labor and Welfare of Japan.

Acknowledgements

We are grateful to A. Ishii and A. Matsuo in our laboratory for their critical discussions. Thanks are also due to K. Imai (Wakayama Prefectural Center, Wakayama) for providing us with RSV, to T. Taniguchi (University of Tokyo, Tokyo), T. Fujita (Kyoto University, Kyoto), K. Miyake (University of Tokyo, Tokyo), M. Nakanishi (The Nagoya City University, Nagoya) and T. Maniatis (Harvard University, Boston, MA, USA) for providing their plasmids. Support by Takeda Science Foundation and NorthTec Foundation are gratefully acknowledged.

Abbreviations

DC	dendritic cell
dsRNA	double-stranded RNA
F protein	fusion glycoprotein
G protein	G glycoprotein
IKKε	IκB kinase-related kinase ε
IPS-1	IFN-β promoter stimulator 1
IRF	IFN-regulatory factor
MALP-2	macrophage-activating lipopeptide-2
MAVS	mitochondria antiviral signaling
MDA5	melanoma differentiation-associated gene 5
mDC	monocyte-derived dendritic cell
MOI	multiplicity of infection
MV	measles virus
NF-κB	nuclear factor-κB
p.i.	post-infection
RIG-I	retinoic acid-inducible gene I
RSV	respiratory syncytial virus
sG	soluble G
TBK1	TANK-binding kinase 1
TIR	Toll–IL-1R
TLR	Toll-like receptor
TNF-α	tumor necrosis factor-α

References

1 Ogra, P. L. 2004. Respiratory syncytial virus: the virus, the disease and the immune response. *Paediatr. Respir. Rev.* 5:119.

2 Steinman, R. M. and Hemmi, H. 2006. Dendritic cells: translating innate to adaptive immunity. *Curr. Top. Microbiol. Immunol.* 311:17.

3 Srikiatkhachorn, A. and Braciale, T. J. 1997. Virus-specific CD8+ T lymphocytes downregulate T helper cell type 2 cytokine secretion and pulmonary eosinophilia during experimental murine respiratory syncytial virus infection. *J. Exp. Med.* 186:421.

4 Creagh, E. M. and O'Neill, L. A. 2006. TLRs, NLRs and RLRs: a trinity of pathogen sensors that co-operate in innate immunity. *Trends Immunol.* 27:352.

5 Groskreutz, D. J., Monick, M. M., Powers, L. S., Yarovinsky, T. O., Look, D. C. and Hunninghake, G. W. 2006. Respiratory syncytial virus induces TLR3 protein and protein kinase R, leading to increased double-stranded RNA responsiveness in airway epithelial cells. *J. Immunol.* 176:1733.

6 Liu, P., Jamaluddin, M., Li, K., Garofalo, R., Casola, A. and Brasier, A. 2007. Retinoic acid inducible gene-I mediates early anti-viral

response and Toll-like receptor 3 expression in respiratory syncytial virus-infected airway epithelial cells. *J. Virol.* 81:1401.
7 Rudd, B. D., Burstein, E., Duckett, C. S., Li, X. and Lukacs, N. W. 2005. Differential role for TLR3 in respiratory syncytial virus-induced chemokine expression. *J. Virol.* 79:3350.
8 Hornung, V., Ellegast, J., Kim, S. *et al.* 2006. 5'-Triphosphate RNA is the ligand for RIG-I. *Science* 314:994.
9 Pichlmair, A., Schulz, O., Tan, C. P. *et al.* 2006. RIG-I-mediated antiviral responses to single-stranded RNA bearing 5'-phosphates. *Science* 314:997.
10 Sasai, M., Shingai, M., Funami, K. *et al.* 2006. NAK-associated protein 1 participates in both the TLR3 and the cytoplasmic pathways in Type I IFN induction. *J. Immunol.* 177:8676.
11 Akazawa, T., Ebihara, T., Okuno, M. *et al.* 2007. Antitumor NK activation induced by the Toll-like receptor 3-TICAM-1 (TRIF) pathway in myeloid dendritic cells. *Proc. Natl Acad. Sci. USA* 104:252.
12 Schulz, O., Diebold, S. Ş., Chen, M. *et al.* 2005. Toll-like receptor 3 promotes cross-priming to virus-infected cells. *Nature* 433:887.
13 Oshiumi, H., Matsumoto, M., Funami, K., Akazawa, T. and Seya, T. 2003. TICAM-1, an adaptor molecule that participates in Toll-like receptor 3-mediated interferon-beta induction. *Nat. Immunol.* 4:161.
14 Yamamoto, M., Sato, S., Mori, K. *et al.* 2002. Cutting edge: a novel Toll/IL-1 receptor domain-containing adapter that preferentially activates the IFN-beta promoter in the Toll-like receptor signaling. *J. Immunol.* 169:6668.
15 Oshiumi, H., Sasai, M., Shida, K., Fujita, T., Matsumoto, M. and Seya, T. 2003. TIR-containing adapter molecule (TICAM)-2, a bridging adapter recruiting to toll-like receptor 4 TICAM-1 that induces interferon-beta. *J. Biol. Chem.* 278:49751.
16 Yamamoto, M., Sato, S., Hemmi, H. *et al.* 2003. TRAM is specifically involved in the Toll-like receptor 4-mediated MyD88-independent signaling pathway. *Nat. Immunol.* 4:1144.
17 Matsumoto, M. and Seya, T. 2008. TLR3: interferon induction by double-stranded RNA including poly(I:C). *Adv. Drug Deliv. Rev.* 60:805.
18 Kawai, T., Takahashi, K., Sato, S. *et al.* 2005. IPS-1, an adaptor triggering RIG-I- and Mda5-mediated type I interferon induction. *Nat. Immunol.* 6:981.
19 Meylan, E., Curran, J., Hofmann, K. *et al.* 2005. Cardif is an adaptor protein in the RIG-I antiviral pathway and is targeted by hepatitis C virus. *Nature* 437:1167.
20 Seth, R. B., Sun, L., Ea, C. K. and Chen, Z. J. 2005. Identification and characterization of MAVS, a mitochondrial antiviral signaling protein that activates NF-kappaB and IRF 3. *Cell* 122:669.
21 Xu, L. G., Wang, Y. Y., Han, K. J., Li, L. Y., Zhai, Z. and Shu, H. B. 2005. VISA is an adapter protein required for virus-triggered IFN-beta signaling. *Mol. Cell* 19:727.
22 Takeuchi, O. and Akira, S. 2008. MDA5/RIG-I and virus recognition. *Curr. Opin. Immunol.* 20:17.
23 Honda, K., Yanai, H., Negishi, H. *et al.* 2005. IRF-7 is the master regulator of type-I interferon-dependent immune responses. *Nature* 434:772.
24 Uematsu, S., Sato, S., Yamamoto, M. *et al.* 2005. Interleukin-1 receptor-associated kinase-1 plays an essential role for Toll-like receptor (TLR)7- and TLR9-mediated interferon-[alpha] induction. *J. Exp. Med.* 201:915.
25 Hoshino, K., Sugiyama, T., Matsumoto, M. *et al.* 2006. IkappaB kinase-alpha is critical for interferon-alpha production induced by Toll-like receptors 7 and 9. *Nature* 440:949.
26 Gotoh, B., Komatsu, T., Takeuchi, K. and Yokoo, J. 2001. Paramyxovirus accessory proteins as interferon antagonists. *Microbiol. Immunol.* 45:787.
27 Ramaswamy, M., Shi, L., Varga, S. M., Barik, S., Behlke, M. A. and Look, D. C. 2006. Respiratory syncytial virus nonstructural protein 2 specifically inhibits type I interferon signal transduction. *Virology* 344:328.
28 Collins, P. L. and Mottet, G. 1991. Post-translational processing and oligomerization of the fusion glycoprotein of human respiratory syncytial virus. *J. Gen. Virol.* 72:3095.
29 Kurt-Jones, E. A., Popova, L., Kwinn, L. *et al.* 2000. Pattern recognition receptors TLR4 and CD14 mediate response to respiratory syncytial virus. *Nat. Immunol.* 1:398.
30 Rudd, B. D., Luker, G. D., Luker, K. E., Peebles, R. S. and Lukacs, N. W. 2007. Type I interferon regulates respiratory virus infected dendritic cell maturation and cytokine production. *Viral Immunol.* 20:531.
31 Levine, S., Klaiber-Franco, R. and Paradiso, P. R. 1987. Demonstration that glycoprotein G is the attachment protein of respiratory syncytial virus. *J. Gen. Virol.* 68:2521.
32 Bukreyev, A., Whitehead, S. S., Murphy, B. R. and Collins, P. L. 1997. Recombinant respiratory syncytial virus from which the entire SH gene has been deleted grows efficiently in cell culture and exhibits site-specific attenuation in the respiratory tract of the mouse. *J. Virol.* 71:8973.
33 Hendricks, D. A., Baradaran, K., McIntosh, K. and Patterson, J. L. 1987. Appearance of a soluble form of the G protein of respiratory syncytial virus in fluids of infected cells. *J. Gen. Virol.* 68:1705.
34 Tripp, R. A. 2004. Pathogenesis of respiratory syncytial virus infection. *Viral Immunol.* 17:165.
35 Nishiguchi, M., Matsumoto, M., Takao, T. *et al.* 2001. Mycoplasma fermentans lipoprotein M161Ag-induced cell activation is mediated by Toll-like receptor 2: role of N-terminal hydrophobic portion in its multiple functions. *J. Immunol.* 166:2610.
36 Ebihara, T., Masuda, H., Akazawa, T. *et al.* 2007. NKG2D ligands are induced on human dendritic cells by TLR ligand stimulation and RNA virus infection. *Int. Immunol.* 19:1145.
37 Peret, T. C., Hall, C. B., Schnabel, K. C., Golub, J. A. and Anderson, L. J. 1998. Circulation patterns of genetically distinct group A and B strains of human respiratory syncytial virus in a community. *J. Gen. Virol.* 79:2221.
38 Matsumoto, M., Seya, T. and Nagasawa, S. 1992. Polymorphism and proteolytic fragments of granulocyte membrane cofactor protein (MCP, CD46) of complement. *Biochem. J.* 281:493(Pt 2).
39 Yoneyama, M. and Fujita, T. 2007. Function of RIG-I-like receptors in antiviral innate immunity. *J. Biol. Chem.* 282:15315.
40 Maher, C. F., Hussell, T., Blair, E., Ring, C. J. and Openshaw, P. J. 2004. Recombinant respiratory syncytial virus lacking secreted glycoprotein G is attenuated, non-pathogenic but induces protective immunity. *Microbes Infect.* 6:1049.
41 Funami, K., Sasai, M., Oshiumi, H., Seya, T. and Matsumoto, M. 2008. Homo-oligomerization is essential for Toll/Interleukin-1 receptor domain-containing adaptor molecule-1-mediated NF-kB and IRF-3 activation. *J. Biol. chem.* 283:18283.
42 Carty, M., Goodbody, R., Schroder, M., Stack, J., Moynagh, P. N. and Bowie, A. G. 2006. The human adaptor SARM negatively regulates adaptor protein TRIF-dependent Toll-like receptor signaling. *Nat. Immunol.* 7:1074.
43 Takaoka, A. and Taniguchi, T. 2003. New aspects of IFN-alpha/beta signalling in immunity, oncogenesis and bone metabolism. *Cancer Sci.* 94:405.
44 Ryzhakov, G. and Randow, F. 2007. SINTBAD, a novel component of innate antiviral immunity, shares a TBK1-binding domain with NAP1 and TANK. *EMBO J.* 26:3180.
45 Olszewska-Pazdrak, B., Casola, A., Saito, T. *et al.* 1998. Cell-specific expression of RANTES, MCP-1, and MIP-1alpha by lower airway epithelial cells and eosinophils infected with respiratory syncytial virus. *J. Virol.* 72:4756.
46 Panuska, J. R., Merolla, R., Rebert, N. A. *et al.* 1995. Respiratory syncytial virus induces interleukin-10 by human alveolar macrophages. Suppression of early cytokine production and implications for incomplete immunity. *J. Clin. Invest.* 96:2445.
47 Tsutsumi, H., Matsuda, K., Sone, S., Takeuchi, R. and Chiba, S. 1996. Respiratory syncytial virus-induced cytokine production by neonatal macrophages. *Clin. Exp. Immunol.* 106:442.
48 Polack, F. P., Irusta, P. M., Hoffman, S. J. *et al.* 2005. The cysteine-rich region of respiratory syncytial virus attachment protein inhibits innate immunity elicited by the virus and endotoxin. *Proc. Natl Acad. Sci. USA* 102:8996.
49 Li, K., Foy, E., Ferreon, J. C. *et al.* 2005. Immune evasion by hepatitis C virus NS3/4A protease-mediated cleavage of the Toll-like receptor 3 adaptor protein TRIF. *Proc. Natl Acad. Sci. USA* 102:2992.
50 O'Neill, L. A. and Bowie, A. G. 2007. The family of five: tIR-domain-containing adaptors in Toll-like receptor signalling. *Nat. Rev. Immunol.* 7:353.

THE JOURNAL OF BIOLOGICAL CHEMISTRY VOL. 283, NO. 33, pp. 22787–22794, August 15, 2008

Modulation of Double-stranded RNA Recognition by the N-terminal Histidine-rich Region of the Human Toll-like Receptor 3*[S]

Received for publication, March 24, 2008, and in revised form, May 20, 2008 Published, JBC Papers in Press, June 10, 2008, DOI 10.1074/jbc.M802284200

Kotaro Fukuda[‡1], Tomoya Watanabe[‡], Takashi Tokisue[‡], Tadayuki Tsujita[§], Satoshi Nishikawa[¶], Tsunemi Hasegawa[‡], Tsukasa Seya[§], and Misako Matsumoto[§]

From the [‡]Department of Material and Biological Chemistry, Faculty of Science, Yamagata University, Yamagata 990-8560, Japan, the [§]Department of Microbiology and Immunology, Graduate School of Medicine, Hokkaido University, Kita-ku, Sapporo 060-8638, Japan, and the [¶]Age Dimension Research Center, National Institute of Advanced Industrial Science and Technology, Tsukuba 305-8566, Japan

Toll-like receptors (TLRs) are an essential component of the innate immune response to microbial pathogens. TLR3 is localized in intracellular compartments, such as endosomes, and initiates signals in response to virus-derived double-stranded RNA (dsRNA). The TLR3 ectodomain (ECD), which is implicated in dsRNA recognition, is a horseshoe-shaped solenoid composed of 23 leucine-rich repeats (LRRs). Recent mutagenesis studies on the TLR3 ECD revealed that TLR3 activation depends on a single binding site on the nonglycosylated surface in the C-terminal region, comprising H539 and several asparagines within LRR17 to -20. TLR3 localization within endosomes is required for ligand recognition, suggesting that acidic pH is the driving force for TLR3 ligand binding. To elucidate the pH-dependent binding mechanism of TLR3 at the structural level, we focused on three highly conserved histidine residues clustered at the N-terminal region of the TLR3 ECD: His^{39} in the N-cap region, His^{60} in LRR1, and His^{108} in LRR3. Mutagenesis of these residues showed that His^{39}, His^{60}, and His^{108} were essential for ligand-dependent TLR3 activation in a cell-based assay. Furthermore, dsRNA binding to recombinant TLR3 ECD depended strongly on pH and dsRNA length and was reduced by mutation of His^{39}, His^{60}, and His^{108}, demonstrating that TLR3 signaling is initiated from the endosome through a pH-dependent binding mechanism, and that a second dsRNA binding site exists in the N-terminal region of the TLR3 ECD characteristic solenoid. We propose a novel model for the formation of TLR3 ECD dimers complexed with dsRNA, which incorporates this second binding site.

Mammalian Toll-like receptors (TLRs)[2] play an essential role in the innate immune response to molecular patterns associated with microbial pathogens. To date, more than 10 functional TLRs have been reported in humans and in mice (1). All TLRs are type I integral membrane glycoproteins composed of an ectodomain (ECD) containing varying numbers of leucine-rich repeats (LRRs) linked by a transmembrane domain to a cytoplasmic signaling Toll/IL-1 receptor (TIR) domain. TLR ECDs are responsible for ligand binding; specific ligands derived from bacterial and viral constituents and their respective TLRs have been identified, including lipoteichoic acid (TLR2), lipopolysaccharide (TLR4), flagellin (TLR5), single-stranded RNA (TLR7 and TLR8), and unmethylated CpG DNA motifs (TLR9) (1). The binding of a ligand to a TLR initiates a series of signaling processes that activate and mediate innate and adaptive immune responses (2). The basic mechanism of TLR signaling is thought to involve ligand-induced dimerization (3).

TLR3 is activated by polyinosinic-polycytidylic acid (poly(I:C)), an analog of double-stranded RNA (dsRNA), as well as by viral infection-associated dsRNAs (4). TLR3 is quite distinct from other TLRs in that it is not dependent on myeloid differentiation factor 88 for signaling. Upon ligand binding, the TLR3 TIR domain recruits the intracellular adaptor molecule TICAM-1, also known as TRIF (TIR-containing adaptor inducing IFN-β) (5, 6). The recruitment of this adaptor leads to the production of antiviral cytokines, such as IFN-β. TLR3 is specifically expressed in immune cells, such as conventional dendritic cells and natural killer cells, as well as in fibroblasts and intestinal epithelial cells (1, 7–9).

The crystal structure of the human TLR3 ECD was recently elucidated by two groups (10, 11). The TLR3 ECD is a horseshoe-shaped solenoid composed of 23 LRRs, which is capped on both ends by characteristic N- and C-terminal structures, and its surface is extensively modified with *N*-linked glycans. However, one surface of the LRR solenoid is free from glycosylation, and the charge properties and two loops protruding from LRR12 and LRR20 on this surface are predicted to be involved in TLR3 function. Recent mutagenesis studies on the TLR3 ECD revealed that a single binding site is present on the nonglycosylated surface near the C terminus. This binding site includes His^{539} and several asparagines in LRR17 to -20 and is essential for TLR3 activation, suggesting a model for TLR3 recognition of dsRNA and the formation of a signaling complex (12–14).

* The costs of publication of this article were defrayed in part by the payment of page charges. This article must therefore be hereby marked "*advertisement*" in accordance with 18 U.S.C. Section 1734 solely to indicate this fact.

[S] The on-line version of this article (available at http://www.jbc.org) contains supplemental Tables S1 and S2.

[1] To whom correspondence should be addressed. Tel.: 81-23-628-4580; Fax: 81-23-628-4604; E-mail: kotaro.f@sci.kj.yamagata-u.ac.jp.

[2] The abbreviations used are: TLR, Toll-like receptor; ECD, ectodomain; LRR, leucine-rich repeat; TIR, Toll/interleukin-1 receptor; poly(I:C), polyinosinic-polycytidylic acid; siRNA, small interfering RNA; dsRNA, double-stranded RNA; HEK, human embryonic kidney; QCM, quartz crystal microbalance; MES, 4-morpholineethanesulfonic acid.

Because the inhibition of endosomal acidification abrogates poly(I:C)-driven TLR3 activation, TLR3 is thought to be localized in intracellular compartments, such as endosomes (8). Indeed, a recent report confirmed that TLR3 associates with c-Src tyrosine kinase on endosomes to initiate antiviral signaling (15). It is therefore likely that TLR3, as well as the nucleic acid-recognizing TLRs, TLR7, TLR8 (16), and TLR9 (17), resides in the endosomal membrane and that binding of each TLR to its ligand occurs in the endosomal compartment. The intracellular localization of nucleic acid-sensing TLRs seems to discriminate between self and nonself nucleic acids (18). In addition to this function, several studies have also shown that an acidic pH within endosomes is required for TLR3 recognition of dsRNA and subsequent downstream receptor signaling (13, 19).

To understand the mechanisms underlying TLR3 function and intracellular localization at the structural level, we focused our attention on conformational changes in the receptor ectodomain of TLR3, especially the ionization of histidine side chains. Because one pK_a of histidine is 6.0, protonation of this group within endosomes can generate an ionic attraction to the negatively charged phosphate backbone of dsRNA. If this hypothesis is correct, then the highly conserved histidine residues clustered in the N-terminal region of the TLR3 ECD, namely His^{39} in the N-cap region, His^{60} in LRR1, and His^{108} in LRR3, may play a key role in TLR3 function in acidified endosomes.

Here, we demonstrate that His^{39}, His^{60}, and His^{108} are indeed critical for human TLR3 activation and direct binding to dsRNA. This indicates that, in addition to the C-terminal binding site, there is a second dsRNA binding site in the N-terminal region of the TLR3 ECD characteristic solenoid. Based on these data, we propose a novel model for the formation of TLR3 ECD dimers complexed with dsRNA.

EXPERIMENTAL PROCEDURES

Cell Culture—For the expression of plasmids encoding human TLR3 and its mutants, HEK293 (human embryonic kidney) cells were used and cultured in DMEM cell culture medium (Gibco) supplemented with 10% heat-inactivated fetal bovine serum (Biosource) and antibiotics (penicillin/streptomycin). Sf21 cells used for baculovirus generation and protein expression were grown in suspension culture in Sf-900 II SFM (Gibco) supplemented with 10% heat-inactivated fetal bovine serum (JRH Biosciences) and antibiotics (penicillin/streptomycin and gentamicin).

Plasmids Carrying Wild-type TLR3 and TLR3 ECD—pEFBOS/TLR3, which consists of a human TLR3 cDNA cloned into the mammalian expression vector pEFBOS, was previously described (20). To obtain the recombinant TLR3 ECD protein with the Bac-to-Bac baculovirus expression system (Invitrogen), a construct for the human TLR3 extracellular domain (residues 28–703) was generated by PCR using pEFBOS/TLR3 as a template and a 5′ primer encoding a HindIII site and a 3′ primer encoding a His_6 tag, STOP codon, and HindIII site. The PCR product was cloned into the HindIII site of pFastBac1/rtTLR5S (21), which contains a pFastBac1 donor plasmid backbone, resulting in the construction of pFastBac/TLR3-ECD. The protein expressed from pFastBac/TLR3-ECD contains the preprotrypsin secretion signal sequence and a FLAG tag at the N terminus.

Site-directed Mutagenesis—Mutations were introduced by PCR-mediated, site-directed mutagenesis using essentially the same procedure as described previously (22). Human TLR3 cDNA in pEFBOS/TLR3 was mutated to produce eight mutant plasmids for a reporter gene assay: H39A, H39E, H60A, H60E, H108A, H108E, H539A, and H539E. To generate the four recombinant mutant proteins rH39A, rH60A, rH108A, and rH108E, a cDNA of the human TLR3 ECD in pFastBac/TLR3-ECD was mutated. The mutagenic primers used to mutate human TLR3 are listed in the supplemental materials (Table S1). The mutated DNA sequences were confirmed by sequencing with an Applied Biosystems model 3100A automatic sequencer (Applied Biosystems).

Expression and Purification of Recombinant TLR3 ECD and Its Mutants—Recombinant human TLR3 ECD protein (TLR3-ECD) was obtained using the Bac-to-Bac baculovirus expression system (Invitrogen). To generate the bacmid DNA encoding the TLR3 ECD, *Escherichia coli* DH10Bac cells were transformed with the recombinant donor plasmid pFastBac/TLR3-ECD. The isolated recombinant bacmid DNA was then transfected into Sf21 cells with UniFECTOR (B-Bridge International, San Jose, CA) to generate the recombinant baculoviruses. To express TLR3-ECD, a suspension culture of Sf21 cells in Sf-900 II SFM (Gibco) was infected by the recombinant baculoviruses, and the cell culture supernatant was harvested 5 days after infection. Subsequently, TLR3-ECD was purified using a HiTrap chelating column (5 ml size; GE Healthcare) at 4 °C and analyzed by 8% SDS-PAGE. Protein-containing fractions were pooled and dialyzed in TNE buffer (10 mM Tris-HCl (pH 7.6), 50 mM NaCl, 1 mM EDTA (pH 8.0)). The dialyzed pool was concentrated using YM-50 (Millipore Corp., Bedford, MA), and TLR3-ECD was identified by immunoblotting with both anti-FLAG tag and anti-His_6 tag antibodies. The four recombinant TLR3-ECD mutant proteins (rH39A, rH60A, rH108A, and rH108E) were also expressed and purified by the same procedure. This procedure produced about 50 μg of recombinant protein from 500 ml of culture medium.

RNA and DNA Preparations—For the production of siRNA and $dsRNA_{40}$, two transcription templates were generated by PCR by using two respective sets of primers (Table S2), which contained T7 RNA promoter sequences on each end of the template. Subsequently, siRNA and $dsRNA_{40}$ were transcribed using a T7 AmpliScribe kit (Epicenter Technologies) with [α-^{32}P]CTP. Following *in vitro* transcription, siRNA was prepared according to the instructions for the Silencer siRNA Construction Kit (Ambion). After *in vitro* transcription, annealed $dsRNA_{40}$ was purified in an 8% native polyacrylamide gel. Corresponding, respective sense and antisense strands were used as follows: siRNA, 5′-CCUGUUCCAUGGCCAACACUU-3′ and 5′-GUGUUGGCCAUGGAACAGGUU-3′; $dsRNA_{40}$, 5′-GGGAGACAGGCCUGUUCCAUGGCCAACACGUUUGUCUCCC-3′ and 5′-GGGAGACAAACGUGUUGGCCAUGGAACAGGCCUGUCUCCC-3′. The respective sense and antisense strands of $dsRNA_{48}$, 5′-UCGAGACAGUCACAGUAUCCUCCAGCCUUACAGCCAAGUAUGAGAGCU-3′ and 5′-AGCUCUCAUACUUGGCUGUAAGGCUGGAGGAUACUGUG-

TABLE 1

Analysis of the interaction between TLR3 ECD and nucleic acids under different pH conditions

The binding of TLR3-ECD (20, 50, or 100 nM) to siRNA, $dsRNA_{40}$, $dsRNA_{48}$, rC_{30}, $dsDNA_{40}$, and dC_{30} was evaluated using a filter binding assay as described under "Experimental Procedures." The concentration of ^{32}P-labeled RNA and DNA was 10 nM for each binding reaction. Each value is the mean ± S.D. of three independent experiments. ND, not detected.

TLR3-ECD	Binding					
	siRNA	$dsRNA_{40}$	$dsRNA_{48}$	rC_{30}	$dsDNA_{40}$	dC_{30}
nM	%	%	%	%	%	%
pH 4.2						
20	13 ± 0.3	23 ± 0.8	24 ± 2.4	9.4 ± 0.3	9.2 ± 0.1	3.2 ± 0.8
50	18 ± 0.7	22 ± 2.8	23 ± 2.0	10 ± 0.6	8.4 ± 0.2	4.8 ± 1.0
100	21 ± 1.0	19 ± 2.0	21 ± 0.4	11 ± 1.5	6.9 ± 0.9	5.9 ± 0.3
pH 5.0						
20	2.4 ± 0.6	18 ± 0.9	20 ± 1.0	2.9 ± 0.7	3.8 ± 0.3	2.6 ± 1.0
50	5.7 ± 0.2	19 ± 2.2	22 ± 1.3	5.3 ± 0.1	4.3 ± 0.2	2.3 ± 0.6
100	8.8 ± 0.3	21 ± 3.3	24 ± 0.9	7.1 ± 1.2	5.2 ± 0.1	3.1 ± 0.6
pH 6.0						
20	ND	1.8 ± 0.4	1.7 ± 0.3	ND	ND	1.2 ± 0.4
50	ND	3.4 ± 0.4	5.7 ± 1.9	ND	ND	1.9 ± 0.9
100	ND	8.3 ± 0.7	10 ± 0.1	ND	ND	2.3 ± 0.7
pH 7.6						
20	ND	ND	2.0 ± 0.3	ND	ND	2.2 ± 1.8
50	ND	0.1 ± 0.1	2.7 ± 0.3	ND	ND	1.6 ± 0.3
100	ND	0.2 ± 0.1	3.0 ± 0.3	ND	ND	2.0 ± 0.4

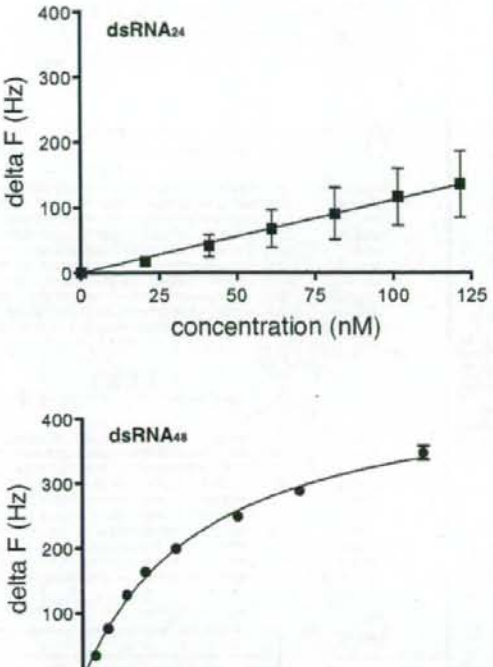

FIGURE 1. **Affinity of TLR3-ECD to $dsRNA_{24}$ and $dsRNA_{48}$.** To investigate the effect of dsRNA length on TLR3 ECD binding at pH 5.0, QCM analysis was performed as described under "Experimental Procedures." TLR3-ECD was injected stepwise into the incubation chamber containing the $dsRNA_{24}$- or $dsRNA_{48}$-coated sensor tip to achieve various concentrations of TLR3-ECD ($dsRNA_{24}$-immobilized QCM, 0–121 nM; $dsRNA_{48}$- immobilized QCM, 0–52.5 nM). The frequency change (*delta F*; Hz) of the dsRNA-immobilized QCM was analyzed, and two binding curves, TLR3-ECD to $dsRNA_{24}$ (*closed squares*) and $dsRNA_{48}$ (*closed circles*), were plotted. Each value is the mean ± S.D. of three independent experiments. The apparent dissociation constant (K_D) calculated for $dsRNA_{48}$ was 19 ± 0.9 nM, but the K_D for $dsRNA_{24}$ could not be determined.

ACUGUCUCGA-3′, were purchased as a duplex RNA from Sigma-Aldrich Japan K.K. The single-stranded RNA of rC_{30} was synthesized using an automated DNA/RNA synthesizer (model 394; ABI). The $dsDNA_{40}$, with a sequence identical to that of $dsRNA_{40}$, was amplified by overlapped-PCR with primers 5′-GGGAGACAGGCCTGTTCCATGGCCA-3′ and 5′-GGGAGACAAACGTGTTGGCCATGGA-3′. The single-stranded DNA of dC_{30} was purchased from Texas Genomics Japan Co. Ltd. All $dsRNA_{48}$, rC_{30}, $dsDNA_{40}$, and dC_{30} were labeled at the 5′-end with [γ-^{32}P]ATP by using T4 polynucleotide kinase.

For the quartz crystal microbalance (QCM) analysis, the respective sense and antisense strands of $dsRNA_{24}$ (5′-end-biotinylated), 5′-CGUAGACAGUCACAGAAUGCUCCA-3′ and 5′-UGGAGCAUUCUGUGACUGUCUACG-3′, and 5′-end-biotinylated $dsRNA_{48}$ were purchased as duplex RNAs from Sigma-Aldrich Japan K.K.

Reporter Gene Assay—HEK293 cells were seeded in 24-well plates (5×10^5 cells/well). Twenty-four hours later, Lipofectamine 2000 (Invitrogen) was used to transiently transfect the cells with pEFBOS/TLR3 or TLR3 mutant expression vectors (0.1 μg) together with a p125-luc reporter (0.1 μg) and a *Renilla* luciferase reporter (0.25 ng). The total amount of transfected plasmid (0.8 μg) was held constant by supplementing with empty vector as needed. Twenty-four hours after transfection, the medium was replaced with fresh medium containing poly(I:C) (10 μg/ml), and the cells were incubated for an additional 6 h. Cells were collected and washed twice with 1 ml of phosphate-buffered saline. The collected cells were lysed using passive lysis buffer (Promega), and the cell lysates were assayed for dual luciferase activities (Promega). Data are expressed as mean relative stimulation ± S.D. for a representative experiment from three independent experiments, performed in triplicate.

Western Blots—HEK293 cells were transiently transfected with target expression vector (0.8 μg) as described above. After 24 h, the cells were collected, washed three times with 1 ml of phosphate-buffered saline, and suspended with lysis buffer (20 mM Tris-HCl (pH 7.4), 150 mM NaCl, 10 mM EDTA (pH 7.4), 1% Nonidet P-40, 25 mM iodoacetamide, 2 mM phenylmethylsulfonyl fluoride) supplemented with Complete Protease Inhibitor (Roche Applied Science). After incubation on ice for 30 min, the lysates were centrifuged, and the supernatants were obtained. The concentration of the supernatants was determined using a protein assay kit (Bio-Rad), and equal amounts of protein were subjected to 7.5% SDS-PAGE. Separated samples were blotted onto polyvinylidene difluoride membrane (Millipore) and probed with a mouse anti-TLR3 antibody (IMG315A; Imegenex Inc.). Horseradish peroxidase-conjugated goat anti-mouse antibody (Biosource) was used as a secondary antibody. Detection of horseradish peroxidase was carried out using a chemiluminescent horseradish peroxidase substrate (Millipore).

Filter Binding Analysis—To analyze the ability of TLR3 to bind siRNA, $dsRNA_{40}$, $dsRNA_{48}$, rC_{30}, $dsDNA_{40}$, and dC_{30},

each ^{32}P-labeled RNA and DNA (10 nM) was incubated with TLR3-ECD (20, 50, or 100 nM) in 50 μl of binding buffer (2 mM HEPES-NaOH (pH 7.6) and 5 mM MES-NaOH (pH 4.2, 5.0, or 6.0) with 100 mM NaCl and 3 mM $MgCl_2$) at 37 °C for 1 h. To evaluate the binding of TLR3-ECD mutants, $dsRNA_{40}$ (10 nM) was incubated with mutants (20 nM) in 50 μl of binding buffer

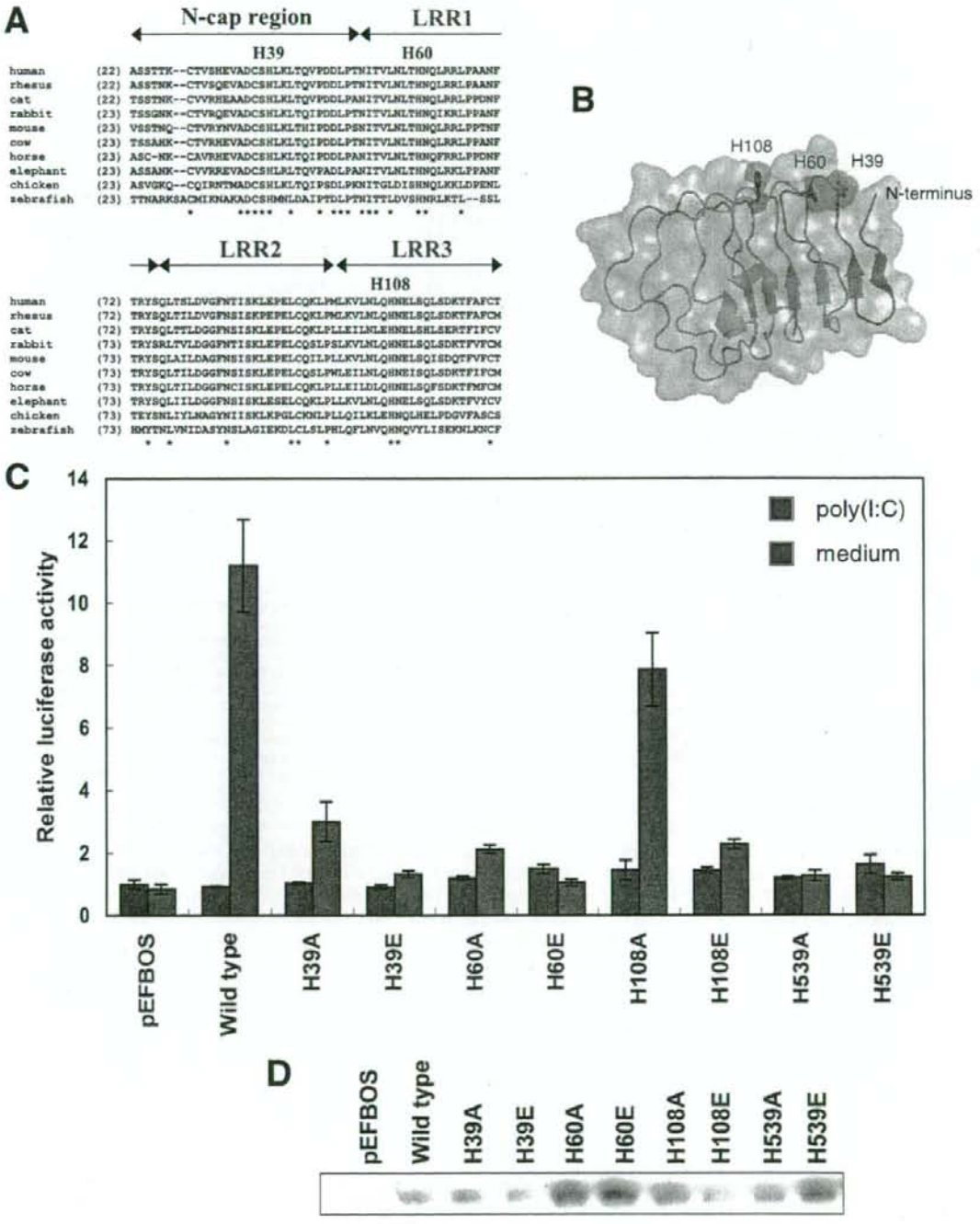

(pH 5.0) as above. The protein-RNA complex was separated by filtration on a nitrocellulose filter (HAWP filter, 0.45 μm; Millipore) fitted in a pop top filter holder (Nucleopore), followed by a wash with 1 ml of binding buffer. Radioactivity remaining on the filter was measured using a BAS2000 image analyzer (Fuji-Film), and the amount of RNA bound to TLR3-ECD or mutants was calculated as a percentage of the RNA input prior to filtration.

QCM Analysis—QCM measurements were performed with a 27-MHz Affinix Q QCM (Initium Co.). The QCM sensor tips were directly immobilized with NeutrAvidin (100 μg/ml; Pierce) in HEPES-NaOH (20 mM, pH 7.6) and NaCl (200 mM) for 12 h at 4 °C. After washing three times with H_2O, the sensor tips were stirred (1000 rpm) at 25 °C in phosphate-buffered saline (1.5 ml) in an incubation chamber. 5′-End biotinylated $dsRNA_{24}$ or $dsRNA_{48}$ (100 pmol) was added to the incubation chamber. To prevent nonspecific interactions between the sensor tip and proteins, phosphate-buffered saline was exchanged with a blocking solution (5 mM MES-NaOH (pH 5.0), 100 mM NaCl, 3 mM $MgCl_2$, and 0.4% Block-Ace Powder (Dainippon Pharma)). TLR3-ECD was then injected stepwise into the incubation chamber containing the immersed dsRNA-coated sensor tip. The binding affinity was indicated by QCM frequency changes recorded by Affinix Q version 1.53 software (Initium), and the disassociation constant (K_D) was calculated with Prism 5 version 5.0a software (Graph Pad Software Inc.).

RESULTS

Importance of Low pH and dsRNA Length for TLR3 ECD Binding—To study the molecular recognition events and biochemical interactions between TLR3 and dsRNA, we first examined the effect of pH on the binding of recombinant TLR3 ECD (TLR3-ECD) to dsRNA. A filter binding assay for TLR3-ECD (20, 50, or 100 nM) was carried out with siRNA, $dsRNA_{40}$, and $dsRNA_{48}$ (10 nM) at pH 4.2–7.6 (Table 1). Binding to TLR3-ECD was undetectable or slight at pH 6.0 and 7.6. However, all dsRNAs bound strongly at lower pH, particularly at pH 4.2. Similar binding patterns were observed for $dsRNA_{40}$ and $dsRNA_{48}$; however, both of these interacted more efficiently with TLR3-ECD than with shorter dsRNA (*i.e.* siRNA).

To examine whether TLR3-ECD could discriminate between single-stranded RNA and dsRNA structures *in vitro*, a filter binding assay was conducted using single-stranded RNA of rC_{30} under the same conditions. Although no detectable binding complex was detected at pH 6.0 or 7.6, binding of rC_{30} at pH 4.2 or 5.0 was moderate compared with the strong binding of $dsRNA_{40}$ (Table 1). Given the preference of TLR3-ECD for dsRNA, the same approach was used to evaluate whether TLR3-ECD could recognize a DNA structure. TLR3-ECD formed a complex with $dsDNA_{40}$, which encoded a sequence identical to that of $dsRNA_{40}$, and the binding was sensitive to pH (Table 1). Although $dsDNA_{40}$ binding was inefficient at pH 6.0 or 7.6, it was moderate at lower pH. Binding of $dsDNA_{40}$ at pH 4.2 and 5.0 was markedly reduced compared with that of $dsRNA_{40}$. The binding of TLR3-ECD to the single-stranded DNA of dC_{30} was much weaker than that to $dsDNA_{40}$ and was not dependent on acidic pH (Table 1). Taken together, these results suggest that the interaction of TLR3-ECD with nucleic acids, especially with dsRNA, is significantly dependent on acidic pH.

We used QCM to more directly characterize the effects of dsRNA length on TLR3 ECD binding in an acidic environment. This highly sensitive QCM technique detects solution phase protein-nucleic acid interactions by monitoring the linear decrease of the emitted frequency, which occurs with increasing mass on the QCM sensor tip. When the $dsRNA_{48}$-coated sensor tip was used, a positive response was observed at all tested concentrations of TLR3-ECD (0–52.5 nM), with an apparent dissociation constant (K_D) of 19 nM (Fig. 1). Strikingly, when the sensor tip was coated with $dsRNA_{24}$ and higher concentrations of TLR3-ECD were used (0–121 nM), the positive response was dramatically reduced, and the K_D value could no longer be determined (Fig. 1). These results suggest that the interaction of TLR3 ECD with dsRNA highly depends on acidic pH and dsRNA length.

His^{39}, His^{60}, and His^{108} Are Essential for the Ligand-dependent Activation of TLR3—To assess how TLR3 senses acidic pH for binding dsRNA, we focused on three highly conserved histidine residues clustered in the N-terminal region of the TLR3 ECD: His^{39} in the N-cap region, His^{60} in LRR1, and His^{108} in LRR3 (Fig. 2*A*). These histidine residues are located between the concave and nonglycosylated lateral surfaces of the TLR3 ECD structure, and all of their imidazole side chains are exposed on the outside of the protein (Fig. 2*B*). Because one pK_a of histidine is 6.0, a pH change within the endosome from neutral to acidic protonates the imidazole group. This is thought to generate an ionic attraction between the histidine and the negatively charged phosphate backbone of the dsRNA.

To test our hypothesis that the N-terminal histidines are crucial for pH-dependent binding of TLR3 ECD to dsRNA, we constructed the site-specific substitution mutants H39A, H39E, H60A, H60E, H108A, and H108E and carried out a reporter gene assay to analyze how mutations in TLR3 influence TLR3 activation. TLR3-negative HEK293 cells were transiently transfected with wild-type (pEFBOS/TLR3) or mutant

FIGURE 2. **His^{39}, His^{60}, and His^{108} mutants affect TLR3 signaling.** *A*, alignment of the N-terminal region of the human TLR3 ECD with homologous sequences from other species. The alignment begins with Ala^{22} of human TLR3. The conserved histidine residues His^{39}, His^{60}, and His^{108}, which were substituted with alanine or glutamic acid in this study, are indicated by *red letters*. *, residues conserved in all 10 species. NCBI accession numbers for sequences are as follows: human, AAH59372; rhesus, NP_001031762; cat, ABB92548; rabbit, ABB76310; mouse, NP_569054; cow, CAH19227; horse, ABB92546; elephant, ABC95781; chicken, ABL74502; zebrafish, NP_001013287. *B*, N-terminal structure of the human TLR3 ECD. The main chain of the N-cap region and the LRR domain are shown with *blue* and *green ribbon models*, respectively. His^{39}, His^{60}, and His^{108}, located on the glycosylation-free face, are represented by *red sticks*. The molecular surface is represented in *gray*, except for His^{39}, His^{60}, and His^{108}, which are in *red* (Protein Data Bank code 2A0Z). *C*, a reporter gene assay was carried out as described under "Experimental Procedures." HEK293 cells transfected with wild-type or mutant TLR3 were (*red bars*) or were not (*blue bars*) stimulated with 10 μg/ml of poly(I:C). Firefly luciferase activity was normalized to *Renilla* luciferase activity. Relative luciferase units were calculated by dividing the normalized luciferase activity by the result obtained using unstimulated, empty pEFBOS vector. *D*, expression of the wild-type and TLR3 mutants was confirmed by Western blotting as described under "Experimental Procedures." The Western blot was probed with mouse anti-TLR3 antibody IMG315A.

TLR3 expression plasmids together with a reporter plasmid containing a luciferase gene under the control of the human IFN-β promoter; the cells were then stimulated with poly(I:C).

Although H108A failed to substantially abrogate the TLR3-mediated activation of luciferase activity, the H39A, H39E, H60A, H60E, and H108E mutants showed a nearly complete loss of function (Fig. 2*C*). The replacement of the histidine residues with glutamic acid rather than alanine had a stronger effect on TLR3 activation by poly(I:C), especially for His^{108}. This may be due to the ionic repulsion between the glutamic acid introduced at His^{39}, His^{60}, and His^{108} and the negative charge on the phosphate backbone of the dsRNA. The mutants did not regain activity, even when 5-fold higher concentrations of the mutant TLR3 expression plasmids were employed (data not shown). This loss of activity was not due to low expression, since Western blot analysis showed that the expression level of each mutant protein was equal to or greater than that of the wild-type (Fig. 2*D*). Thus, His^{39}, His^{60}, and His^{108} in the N-terminal region of the TLR3 ECD are essential for ligand-dependent activation of TLR3.

Direct Binding between His^{39}, His^{60}, and His^{108} and dsRNA—To elucidate whether these essential histidine residues directly contacted dsRNA, we analyzed the binding between recombinant mutant TLR3 proteins and $dsRNA_{40}$ at acidic pH. Purified TLR3-ECD mutant proteins, rH39A, rH60A, rH108A, and rH108E, were verified by performing 8% SDS-PAGE stained with Coomassie Blue R-250 (Fig. 3*A*). rH108A showed partial loss of binding (about 60% of the wild type) to $dsRNA_{40}$ at pH 5.0 (Fig. 3*C*). In contrast, rH39A, rH60A, and rH108E exhibited remarkably diminished binding to $dsRNA_{40}$ (Fig. 3, *B* and *C*). These observations clearly correlated with the results obtained in the reporter gene assay (Fig. 2*C*). It can therefore be concluded that the loss of function observed in the TLR3 mutants is due to their inability to recognize dsRNA and that His^{39}, His^{60}, and His^{108} are essential for the direct binding of TLR3 to dsRNA at acidic pH.

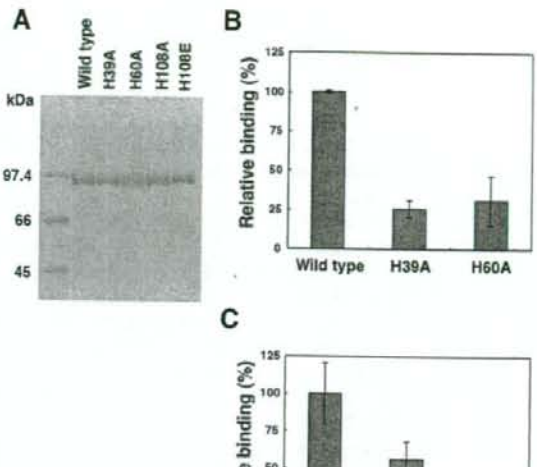

FIGURE 3. **Binding of TLR3-ECD mutants to $dsRNA_{40}$.** *A*, purified TLR3-ECD mutant proteins. Approximately 0.5 μg of wild type and each of the mutant proteins, rH39A, rH60A, rH108A, and rH108E, were loaded on an 8% SDS-PAGE. *B* and *C*, to analyze the binding of TLR3-ECD mutants, ^{32}P-labeled $dsRNA_{40}$ (10 nM) was incubated with TLR3-ECD (wild type), rH39A, rH60A, rH108A, or rH108E (20 nM) in 50 μl of binding buffer (5 mM MES-NaOH (pH 5.0), 100 mM NaCl, and 3 mM $MgCl_2$) at 37 °C for 1 h. A filter binding assay was carried out as described under "Experimental Procedures." To normalize the data, wild-type binding activity was set to 100%. The values ± S.D. are derived from three independent experiments.

DISCUSSION

Mutational analyses have identified several important residues in the TLR3 ECD that are essential for ligand recognition and signal transduction. An impressive report by Bell *et al.* (12) showed that His^{539} and Asn^{541} in LRR20 are crucial for the activation of TLR3. Following this report, Ranjith-Kumar *et al.* (13) identified asparagines in LRR17 to LRR20 that also contribute to TLR3 activation. In this study, we identified three histidine residues, His^{39} in the N-cap region, His^{60} in LRR1, and His^{108} in LRR3, that are essential for human TLR3 activation and ligand binding. In contrast with our results, Bell *et al.* (12) reported that H39A and H60A had no effect on TLR3 activation. This discrepancy may be due to sensitivity differences in the cell-based assay systems used, as observed for the His^{539} substitution mutants. According to their report, the H539E mutation, but not the H539A mutation, resulted in almost complete loss of function. However, in our assay system, both H539E and H539A showed significant effects on TLR3 activation (Fig. 2*C*).

Because $dsRNA_{40}$ was bound to TLR3-ECD more efficiently than to the same sequence of $dsDNA_{40}$, we posit that there exists a difference between forms of dsRNA (A-DNA-like form) and dsDNA (B-form) with respect to nucleic acid backbone helical structures and/or recognition of the 2′-OH group in the ribose of dsRNA (Table 1). Indeed, it has been reported that the presence of the ribose 2′-OH group in poly(I:C) is essential for its recognition by TLR3 (20). Furthermore, the efficiency of TLR3-ECD binding to dsRNA was strictly modulated by the acidic pH conditions, as shown in Table 1. These results indicate that His^{539} and the histidine cluster at the N-terminal region might act as pH sensors to recruit dsRNA. Once the imidazole side chains are protonated in an acidic compartment, such as an endosome, the resulting positive electrostatic potential would presumably lead to the interaction of TLR3 with dsRNA. This suggests that TLR3 signaling is initiated from within the endosome, based on a pH-dependent binding mechanism that is regulated by these functional histidine residues. Consistent with this, Ranjith-Kumar *et al.* (13) previously reported observations from a UV cross-linking assay showing that the TLR3 ECD specifically interacts with dsRNA at acidic pH. Furthermore, Bouteiller *et al.* (19) have shown using a chimeric TLR3-CD32 receptor that recognition of dsRNA by TLR3 and subsequent signal transduction require an acidic pH. It is therefore likely that TLR3-dsRNA interactions occur in acidic compartments to activate signal transduction. Histidine residues on other receptors have also been implicated in acid-regulated mechanisms (23, 24). Other nucleic acid-recognizing TLRs, TLR7, TLR8, and TLR9, are localized in acidic compart-

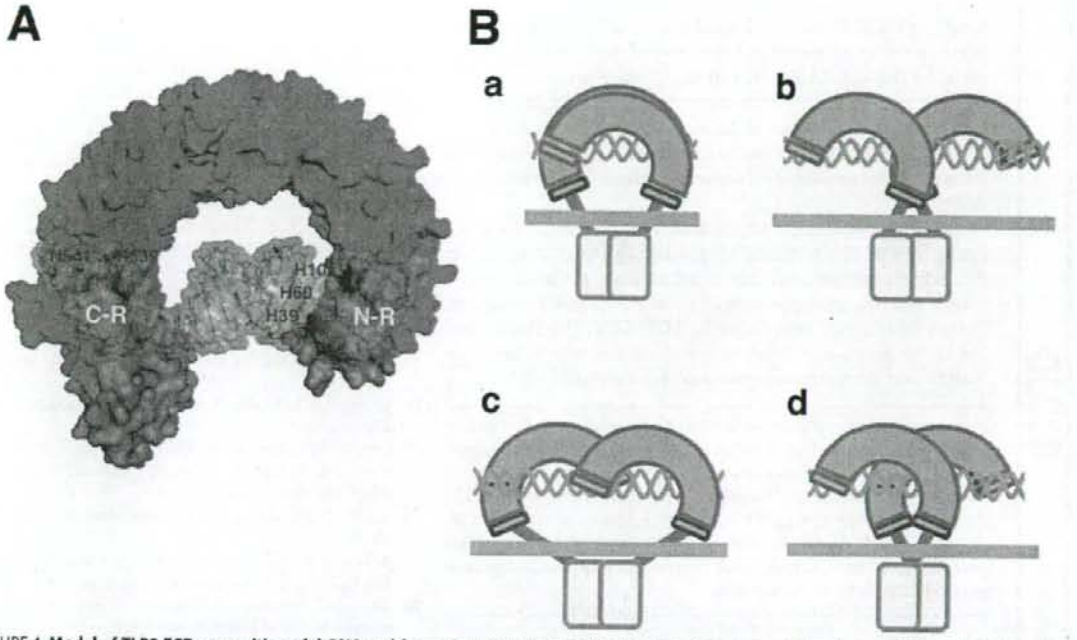

FIGURE 4. **Model of TLR3 ECD recognition of dsRNA and formation of symmetric TLR3 dimers.** *A*, the N-cap region, C-cap region, and LRR domain are represented by *blue*, *magenta*, and *green* surfaces, respectively (Protein Data Bank code 2A0Z). His^{39}, His^{60}, and His^{108} in the N-terminal region (*N-R*) and His^{539} and Asn^{541} in the C-terminal region (*C-R*) are shown in *red* and are involved in the interaction with a dsRNA, 29 bp in length (*gray surface*; Protein Data Bank code 1QC0). Using manual docking performed with PyMOL (version 0.99, DeLano Scientific LLC), we determined that a 29-bp dsRNA can lie across both the N-terminal region and C-terminal region in the TLR3 ECD solenoid and that the minor groove provides the interaction surface for His^{39}, His^{60}, and His^{108}. The interval between the two binding sites is estimated to be two helical turns of dsRNA. *B*, a dsRNA cross-links two molecules of the TLR3 ECD, related by a 180° rotation, resulting in a precisely symmetrical dimer of the TLR3 ECD. Two TLR3 ECD molecules sandwich a dsRNA at two sites in both the N-terminal region and C-terminal region, fixing the dsRNA at four sites. Because the symmetrical arrangement of two TLR3 ECD molecules can be changed by sliding along a dsRNA, it is difficult to determine a single, accurate signaling complex. Two TLR3 ECD molecules can sandwich a dsRNA in both the N-terminal region and C-terminal region (*a*), only the C-terminal region (*b*), or only the N-terminal region (*c*). *d*, the dsRNA is not sandwiched between the N-terminal region or the C-terminal region. The *color scheme* is the same as in *A*. The *yellow boxes* represent the TIR domains.

ments, such as endosomes, indicating that the ligand-binding and signaling of these receptors are also likely to require acidic pH. Indeed, it has been reported that TLR9 interacts with its ligand, nonmethylated CpG DNA, at acidic pH (25).

The basic mechanism of TLR signaling is thought to involve ligand-induced dimerization. In a model proposed by Bell *et al.* (12), the TLR3 ECD contains a single ligand-binding site in LRR20 close to the C terminus, and two TLR3 monomers sandwich a dsRNA in a precisely symmetrical arrangement. Ranjith-Kumar *et al.* (13) proposed a similar architecture for TLR3 ECD complexed with dsRNA, although they suggested a model different from that of Bell *et al.* (12), in which ligand binding to the TLR3 ECD induces dimerization and subsequent TIR domain activation. In this study, we revealed a second histidine-enriched binding site in the N-terminal region of the TLR3 ECD, in addition to the limited C-terminal binding site. We also found that the binding constant of $dsRNA_{24}$ was much higher than that of $dsRNA_{48}$ (Fig. 1). This indicates that the stability of the TLR3-dsRNA complex is affected by the dsRNA length. Although the 24-bp length of dsRNA would be sufficient for TLR3 binding if the ECD contained only the limited C-terminal binding site, the binding constants indicate that $dsRNA_{24}$ affinity for TLR3-ECD is quite low compared with that of $dsRNA_{48}$. Given the approximate distance between the N- and C-terminal binding sites (~30 bp of dsRNA; *gray surface* in Fig. 4*A*), $dsRNA_{48}$, but not $dsRNA_{24}$, is sufficiently long to bridge the distance between the regions. These results, together with the recent report that TLR3 ECD monomers bind cooperatively to dsRNA to form stable dimeric complexes and require a dsRNA length of at least 40–50 bp to bind a single dimmer (26), strongly suggest that there exist two binding sites in the TLR3 ECD, which are both essential for the dsRNA recognition by the TLR3 ECD.

Taking into account all of these data, we determined that a 29-bp length of dsRNA (Fig. 4*A*, *gray surface*) can lie across the two binding sites on the TLR3 solenoid, based on configuration adaptability predicted by a manual docking analysis (Fig. 4*A*). From this analysis, we propose a new model for the formation of symmetric TLR3 dimers (Fig. 4*B*). Given that the N- and C-terminal binding sites appear on the same glycosylation-free face, it would be possible to assemble at least four ternary architectural units, each composed of two TLR3s and a single dsRNA (Fig. 4*B*). A commonly observed feature is that two TLR3 monomers contact a dsRNA via two N- and C-terminal binding sites, so that a dsRNA is fixed at four different positions in a single unit. Although the capability to form dimers in the TIR domain is vital for subsequent signaling, the symmetric arrangement of the two TLR3 molecules can vary along the

length of a dsRNA (see the legend to Fig. 4*B*). Communication between the two nonglycosylated faces of the TLR3 ECD separated by the dsRNA (*e.g.* the loop structure protruding from LRR12), might determine the exact structure of the dimer. Further biochemical analyses or determination of the crystal structure of TLR3 ECD in complex with a dsRNA will be required to determine the precise mechanism by which TLR3 recognizes dsRNA.

Our study with single amino acid mutations in TLR3 demonstrates that the histidine cluster in the N-terminal region functions to recognize dsRNA based on acid-regulated mechanisms, indicating the presence of a second dsRNA binding site in the characteristic solenoid of the TLR3 ECD. This finding has led us to propose a novel dimer structure, which provides insight into the ligand recognition mechanism of TLR3.

Acknowledgments—We thank K. Ito, K. Funami, and E. Takada (Hokkaido University) for technical support with the cell-based experiments. We thank T. Jitsukawa and S. Chiba (ULVAC, Inc.) for technical support with the QCM analysis. We thank F. Nishikawa (AIST) for the preparation of rC_{30}. We also thank S. Miyata, Y. Asanuma, K. Hatakeyama, K. Konno, R. Narita, and R. Tozuka (Yamagata University) for technical support with the construction of wild-type and mutant TLR3 expression plasmids.

REFERENCES

1. Akira, S., Uematsu, S., and Takeuchi, O. (2006) *Cell* **124,** 783–801
2. Iwasaki, A., and Medzhitov, R. (2004) *Nat. Immunol.* **5,** 987–995
3. Gay, N. J., Gangloff, M., and Weber, A. N. (2006) *Nat. Rev. Immunol.* **6,** 693–698
4. Alexopoulou, L., Holt, A. C., Medzhitov, R., and Flavell, R. A. (2001) *Nature* **413,** 732–738
5. Oshiumi, H., Matsumoto, M., Funami, K., Akazawa, T., and Seya, T. (2003) *Nat. Immunol.* **4,** 161–167
6. Yamamoto, M., Sato, S., Mori, K., Hoshino, K., Takeuchi, O., Takeda, K., and Akira, S. (2002) *J. Immunol.* **169,** 6668–6672
7. Matsumoto, M., Kikkawa, S., Kohase, M., Miyake, K., and Seya, T. (2002) *Biochem. Biophys. Res. Commun.* **293,** 1364–1369
8. Matsumoto, M., Funami, K., Tanabe, M., Oshiumi, H., Shingai, M., Seto, Y., Yamamoto, A., and Seya, T. (2003) *J. Immunol.* **171,** 3154–3162
9. Schroder, M., and Bowie, A. G. (2005) *Trends Immunol.* **26,** 462–468
10. Choe, J., Kelker, M. S., and Wilson, I. A. (2005) *Science* **309,** 581–585
11. Bell, J. K., Botos, I., Hall, P. R., Askins, J., Shiloach, J., Segal, D. M., and Davies, D. R. (2005) *Proc. Natl. Acad. Sci. U. S. A.* **102,** 10976–10980
12. Bell, J. K., Askins, J., Hall, P. R., Davies, D. R., and Segal, D. M. (2006) *Proc. Natl. Acad. Sci. U. S. A.* **103,** 8792–8797
13. Ranjith-Kumar, C. T., Miller, W., Xiong, J., Russell, W. K., Lamb, R., Santos, J., Duffy, K. E., Cleveland, L., Park, M., Bhardwaj, K., Wu, Z., Russell, D. H., Sarisky, R. T., Mbow, M. L., and Kao, C. C. (2007) *J. Biol. Chem.* **282,** 7668–7678
14. Takada, E., Okahira, S., Sasai, M., Funami, K., Seya, T., and Matsumoto, M. (2007) *Mol. Immunol.* **44,** 3633–3640
15. Johnsen, I. B., Nguyen, T. T., Ringdal, M., Tryggestad, A. M., Bakke, O., Lien, E., Espevik, T., and Anthonsen, M. W. (2006) *EMBO J.* **25,** 3335–3346
16. Gibbard, R. J., Morley, P. J., and Gay, N. J. (2006) *J. Biol. Chem.* **281,** 27503–27511
17. Latz, E., Schoenemeyer, A., Visintin, A., Fitzgerald, K. A., Monks, B. G., Knetter, C. F., Lien, E., Nilsen, N. J., Espevik, T., and Golenbock, D. T. (2004) *Nat. Immunol.* **5,** 190–198
18. Barton, G. M., Kagan, J. C., and Medzhitov, R. (2006) *Nat. Immunol.* **7,** 49–56
19. de Bouteiller, O., Merck, E., Hasan, U. A., Hubac, S., Benguigui, B., Trinchieri, G., Bates, E. E., and Caux, C. (2005) *J. Biol. Chem.* **280,** 38133–38145
20. Okahira, S., Nishikawa, F., Nishikawa, S., Akazawa, T., Seya, T., and Matsumoto, M. (2005) *DNA Cell Biol.* **24,** 614–623
21. Tsujita, T., Tsukada, H., Nakao, M., Oshiumi, H., Matsumoto, M., and Seya, T. (2004) *J. Biol. Chem.* **279,** 48588–48597
22. Fukuda, K., Morioka, H., Imajou, S., Ikeda, S., Ohtsuka, E., and Tsurimoto, T. (1995) *J. Biol. Chem.* **270,** 22527–22534
23. Rudenko, G., Henry, L., Henderson, K., Ichtchenko, K., Brown, M. S., Goldstein, J. L., and Deisenhofer, J. (2002) *Science* **298,** 2353–2358
24. Doi, T., Kurasawa, M., Higashino, K., Imanishi, T., Mori, T., Naito, M., Takahashi, K., Kawabe, Y., Wada, Y., Matsumoto, A., and Kodama, T. (1994) *J. Biol. Chem.* **269,** 25598–25604
25. Rutz, M., Metzger, J., Gellert, T., Luppa, P., Lipford, G. B., Wagner, H., and Bauer, S. (2004) *Eur. J. Immunol.* **34,** 2541–2550
26. Leonard, J. N., Ghirlando, R., Askins, J., Bell, J. K., Margulies, D. H., Davies, D. R., and Segal, D. M. (2008) *Proc. Natl. Acad. Sci. U. S. A.* **105,** 258–263

Hepatitis C Virus–Infected Hepatocytes Extrinsically Modulate Dendritic Cell Maturation To Activate T Cells and Natural Killer Cells

Takashi Ebihara,[1] Masashi Shingai,[1] Misako Matsumoto,[1] Takaji Wakita,[2] and Tsukasa Seya[1]

Dendritic cell maturation critically modulates antiviral immune responses, and facilitates viral clearance. Hepatitis C virus (HCV) is characterized by its high predisposition to persistent infection. Here, we examined the immune response of human monocyte-derived dendritic cells (MoDCs) to the JFH1 strain of HCV, which can efficiently replicate in cell culture. However, neither HCV RNA replication nor antigen production was detected in MoDCs inoculated with JFH1. None of the indicators of HCV interacting with MoDCs we evaluated were affected, including expression of maturation markers (CD80, 83, 86), cytokines (interleukin-6 and interferon-beta), the mixed lymphocyte reaction, and natural killer (NK) cell cytotoxicity. Strikingly, MoDCs matured by phagocytosing extrinsically-infected vesicles containing HCV-derived double-stranded RNA (dsRNA). When MoDCs were cocultured with HCV-infected apoptotic Huh7.5.1 hepatic cells, there was increased CD86 expression and interleukin-6 and interferon-beta production in MoDCs, which were characterized by the potential to activate NK cells and induce $CD4^+$ T cells into the T helper 1 type. Lipid raft-dependent phagocytosis of HCV-infected apoptotic vesicles containing dsRNA was indispensable to MoDC maturation. Colocalization of dsRNA with Toll-like receptor 3 (TLR3) in phagosomes suggested the importance of TLR3 signaling in the MoDC response against HCV. *Conclusion:* The JFH1 strain does not directly stimulate MoDCs to activate T cells and NK cells, but phagocytosing HCV-infected apoptotic cells and their interaction with the TLR3 pathway in MoDCs plays a critical role in MoDC maturation and reciprocal activation of T and NK cells. (HEPATOLOGY 2008;48:48-58.)

Abbreviations: CPZ, chlorpromazine; CTL, cytotoxic T lymphocyte; DC, dendritic cell; DC-SIGN, dendritic cell-specific intercellular adhesion molecule 3-grabbing nonintegrin; dsRNA, double-stranded RNA; ELISA, enzyme-linked immunosorbent assay; FACS, fluorescence-activated cell sorting; HCV, hepatitis C virus; IFN, interferon; IFNAR, type I IFN-alpha receptor; IL, interleukin; IRF, IFN regulatory factor; MβCD, methyl-beta-cyclodextrin; MDA5, melanoma differentiation associated gene 5; mAb, monoclonal antibody; MoDC, monocyte-derived dendritic cell; MOI, multiplicity of infection; MV, measles virus; NK, natural killer; NKG2D, natural killer group 2, member D; PAMP, pathogen associated molecular pattern; PBMC, peripheral blood mononuclear cells; pDC, plasmacytoid DC; poly I:C, polyinosinic:polycytidylic acid; RIG-I, retinoic acid inducible gene I; RSV, respiratory syncytial virus; RT-PCR, reverse-transcription polymerase chain reaction; siRNA, small interfering RNA; SNARF1, far red immunofluorescence dye; Th1, T helper 1; TLR, Toll-like receptor; TNF, tumor necrosis factor.

From the [1]Department of Microbiology and Immunology, Hokkaido University Graduate School of Medicine, Sapporo, Japan; and [2]Department of Virology II, National Institute of Infectious Diseases, Tokyo, Japan.

Received September 10, 2007; accepted March 11, 2008.

Supported in part by CREST and Innovation, Japan Science and Technology Corporation, the Program of Founding Research Centers for Emerging and Reemerging Infectious Diseases, MEXT, and Grants-in-Aid from the Ministry of Education, Science, and Culture (Specified Project for Advanced Research) and the Ministry of Health, Labor, and Welfare of Japan and the HCV project in National Institute of Health of Japan, and by the Takeda Foundation, Uehara memorial Foundation, Mitsubishi Foundation, Akiyama Foundation, and NorthTec Foundation.

Masashi Shingai is currently affiliated with the Laboratory of Molecular Microbiology, National Institute of Allergy and Infectious Diseases, National Institutes of Health, Bethesda, MD.

Address reprint requests to: Tsukasa Seya, Department of Microbiology and Immunology, Graduate School of Medicine, Hokkaido University, Kita-ku, Sapporo, 060-8638, Japan. E-mail: seya-tu@pop.med.hokudai.ac.jp; fax: 81-11-706-7866.

Published online in Wiley InterScience (www.interscience.wiley.com).

DOI 10.1002/hep.22337

Potential conflict of interest: Nothing to report.

Hepatitis C virus (HCV) is a single-strand, positive-sense RNA virus belonging to the flaviviridae family. HCV develops persistent infection in <70% of infected patients, and eventually causes chronic hepatitis, cirrhosis, and hepatocellular carcinoma in some patients.[1] Once chronic infection is established in patients with HCV, spontaneous viral clearance fails,[1] although how HCV remains persistently infecting the liver is unknown. It has been accepted that successful viral clearance by the host is largely attributed to robust induction of type I interferon (IFN) and antiviral cellular effectors, cytotoxic T lymphocyte (CTL) and natural killer (NK) cells.[2-5] In HCV-infected patients and chimpanzees, type I IFN induction and activation of HCV-specific $CD4^+$ T/$CD8^+$ T cells and NK cells are indeed detected during acute infection.[4-6] However, why these antiviral factors cannot eradicate HCV from most patients is not addressed. Facilities for inducing the antiviral effectors and their role against HCV persistence have not been well determined. A main cause for the deficiency of knowledge on the host response to HCV is the lack of an appropriate model for experimental HCV infection.

Two breakthroughs have now made it possible to investigate the immune response against HCV. First, Toll-like receptors (TLRs) and other innate immune receptors of dendritic cells (DCs) were found to be involved in the host antiviral IFN response, followed by CTL and NK cell activation.[2,7-9] Some reports revealed that HCV proteins participate in the regulation of IFN-inducing innate responses.[10-12] Second, an *in vitro* amplifiable 2a type HCV strain, JFH1, was established by Wakita et al.[13] and Zhong et al.[14] Infection studies for testing HCV replication and the immune response are therefore now feasible *in vitro*.

There are two major subsets of DCs in humans: plasmacytoid DCs (pDCs) expressing TLR7 and TLR9 and myeloid DCs expressing Toll-like receptor 3 (TLR3) for viral RNA/DNA recognition. Cytoplasmic RNA sensors, retinoic acid inducible gene I (RIG-I)-like receptors, also participate in viral RNA recognition and IFN induction.[7] RNA virus infection allows pDCs to induce type I IFN via TLR7.[15] On the contrary, myeloid DCs recognize virus-derived double-stranded RNA (dsRNA) to activate pathways for IFN-beta production and NK/CTL induction.[7-9,16] What happens in the pathway of myeloid DC maturation during HCV infection can now be experimentally followed up in infected cells as the JFH1 strain can be used for *in vitro* infection studies. Hence, we inoculated monocyte-derived (Mo)DCs with JFH1 of HCV.

Here, we show evidence that the JFH1 strain has no direct route for MoDC infection and MoDCs phagocytosing HCV-infected apoptotic vesicles participate in MoDC maturation and reciprocal activation of T cells and NK cells.

Materials and Methods

Cell Lines, Antibodies, and Reagents. Huh7.5.1 cells were kindly provided by Dr. Francis V. Chisari (The Scripps Research Institute, La Jolla, CA), and maintained in Dulbecco's modified Eagle's medium–based medium.[14] Following materials were obtained as indicated: anti-HCV-core monoclonal antibody (mAb; C7-50) from Affinity BioReagents (Golden, CO), mAbs against CD80, CD83, and CD86 from Immunotech (Fullerton, CA), anti-dsRNA mAb (K1) from English & Scientific Consulting Bt (Szirak, Hungary), biotin-conjugated anti-TLR3 mAb from eBioscience (San Diego, CA), fluorescein isothiocyanate–labeled goat anti-mouse immunoglobulin G from American Qualex (San Clemente, CA), Streptavidin Alexa Fluor 594 conjugate and SNARF1 from Molecular Probe (Carlsbad, CA), Methyl-beta-cyclodextrin (MβCD), chlorpromazine (CPZ), and bafilomycin (BAF) from Sigma-Aldrich (St. Louis, MO).

Preparation of Immature MoDCs, NK Cells, and T Cells. $CD14^+$ monocytes and autologous NK cells were isolated from human peripheral blood mononuclear cells (PBMCs) using a MACS system (Miltenyi Biotec, Bergisch Gladbach, Germany).[17] Cells purified by this technique had an average purity of 95%, as assessed by flow cytometry. Immature MoDCs were generated from monocytes using human granulocyte-macrophage colony-stimulating factor (GM-CSF; PeproTech, Rocky Hill, NJ) and interleukin (IL)-4 (PeproTech).[17] Autologous NK cells were stocked in Cell Banker (Diaton, Tokyo, Japan) at −80°C. Allogeneic $CD4^+$ and $CD8^+$ T cells were also negatively isolated by a MACS system (Miltenyi Biotec).

Stimulation of Immature MoDC, Cytokine Assay, Immunofluorescent Staining, and Flow Cytometry. The immature MoDCs (2×10^5) were inoculated with HCV and respiratory syncytial virus (RSV) at a multiplicity of infection (MOI) of one or treated with polyinosinic: polycytidylic acid (poly I:C; 10 μg/mL), and cultured in a 24-well plate. The cells and culture supernatant were harvested at indicated time points for reverse transcription polymerase chain reaction (RT-PCR), fluorescence-activated cell sorting (FACS), and enzyme-linked immunosorbent assay (ELISA; IFN-beta, IFN-gamma; Fujirebio, Inc., Tokyo, Japan; IL-6; BD Biosciences, Franklin Lakes, NJ). In some experiments, immature MoDCs (2×10^5) were cocultured with HCV- or non-infected apoptotic cells (4×10^5). MoDCs were treated with MβCD (1 mM), CPZ (5 μg/mL), and BAF (100

nM) for 1 hour before coculture. The viability of these MoDCs was examined by proidium iodide staining. After 2 days of coculture, the MoDCs were isolated from the apoptotic cells by Ficoll-Paque Plus (GE-Healthcare, Waukesha, WI) using the manufacturer's methods, and used for further analysis to assess MoDC functions. The cell lysates were produced from the apoptotic cells by three freeze/thaw cycles, followed by centrifugation at 15,000 rpm for 5 minutes or by sonication three times for 20 seconds on ice. Total RNA was extracted by Trizol (Invitrogen, Carlsbad, CA) by the manufacturer's methods. MoDCs (5×10^5 cells) were transfected with 0.625 μg total RNA by N-[1-(2,3-Dioleoyloxy)propyl]-N, N, N-trimethylammonium methyl-sulfate (DOTAP; Roche, Mannheim, Germany) and cultured in 24-well plates for 1 day. Huh7.5.1 cells were transfected with poly I:C using Lipofectamine 2000 (Invitrogen) by the manufacturer's methods. ELISA for determination of cytokine levels, flow cytometry, and immunofluorescent staining were performed as reported.[17,18]

Virus Propagation. The method to generate infectious HCV particles was referred to an *in vitro* system using the plasmid pJFH-1.[16] Noninfected cell supernatant was used as noninfected control. The concentrated virus had a titer of 1 to 2×10^6 ffu/mL. A RSV field-isolate strain (RSV2177) was propagated with Hep-2 cells as described.[17] The titer of RSV2177 was determined by 50% tissue culture infective dose (TCID50) with Hep-2 cells.

Real-time PCR Quantification of Positive-Strand and Negative-Strand HCV RNA. Total Trizol-extracted RNA was analyzed by reverse transcription-PCR (RT-PCR) with a modification of the previously described strand-specific rTth RT-PCR method.[19] RT primers for complementary DNA synthesis of positive and negative strand HCV RNA were GTGCACGGTCTACGAGACCT and GAGTGTCGTACAGCCTCCAG, respectively. Positive-strand and negative-strand HCV PCR amplifications were performed using Platinum SYBR Green qPCR SuperMix-UDG (Invitrogen) with 200 nM of paired primers, forward CGGGAGAGCCATAGTGG and reverse AGTACCACAAGGCCTTTCG. The PCR conditions were 95°C for 10 minutes, followed by 40 cycles of 95°C for 15 seconds and 60°C for 1 minute. This PCR method could detect 10 copies of positive-strand or negative-strand HCV.

Induction and Certification of Apoptosis. A total of 1×10^5 Huh7.5.1 cells were plated in a 24-well plate and infected with the JFH1 strain at an MOI of 1. At indicated timed intervals, the infected cells and poly I:C-transfected cells were pretreated with cycloheximide

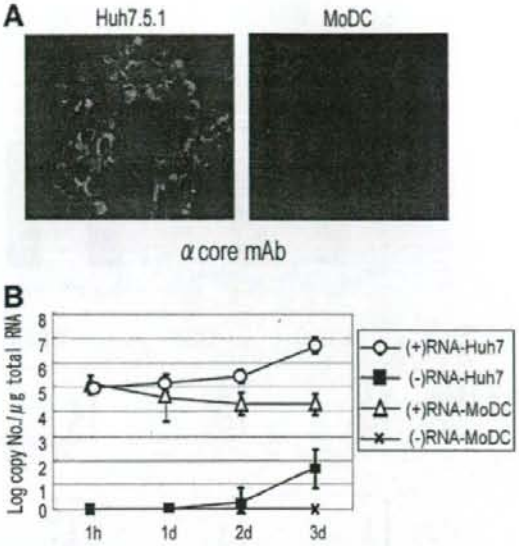

Fig. 1. MoDCs are not permissive for HCV replication. (A) Huh7.5.1 cells and MoDCs were inoculated with HCV at an MOI of 1 and cultured for 3 days. The presence of HCV core antigens was assessed by immunofluorescent staining. (B) Real-time RT-PCR to detect positive-strand and negative-strand HCV RNA. Data show means ± SD from three independent experiments using three different donors.

(20 μg/mL; Sigma) for 30 minutes, followed by tumor necrosis factor (TNF)-alpha (10 ng/mL; Pepro-Tech). The HCV-infected and noninfected apoptotic cells were harvested after another 24-hour culture. Using the HCV-infected apoptotic cells, we examined the presence of HCV core antigens and dsRNA by FACS using anti-HCV core mAb and anti-dsRNA mAb, respectively. Apoptosis was assessed by 4′,6-diamidino-2-phenylindole-staining, DNA fragmentation, and FACS by using fluorescein isothiocyanate–labeled annexin-V and proidium iodide (Roche).[20]

Assay for Lymphocyte Proliferation by MoDC. After 2 days culture of MoDCs with HCV, poly I:C (10 μg/mL), or the apoptotic cells, MoDCs were harvested and treated with mitomycin C (20 μg/mL) in phosphate buffered saline for 45 minutes. For the proliferation assay, the stimulated-MoDCs (1×10^4) were cultured with 1×10^5 allogeneic PBMCs, $CD4^+$ T cells, or $CD8^+$ T cells in U-bottom 96-well plates for 6 days. During the last 24 hours of culturing, [^{3}H]thymidine (1 mCi/well) was added to the culture medium. Then the cells and medium were harvested separately by a cell-harvester, and the radioactivity was measured by a liquid scintillation counter (Aloca, Tokyo, Japan). For the analysis of $CD4^+$ T cell polarization, the stimulated-MoDCs (1×10^4) were

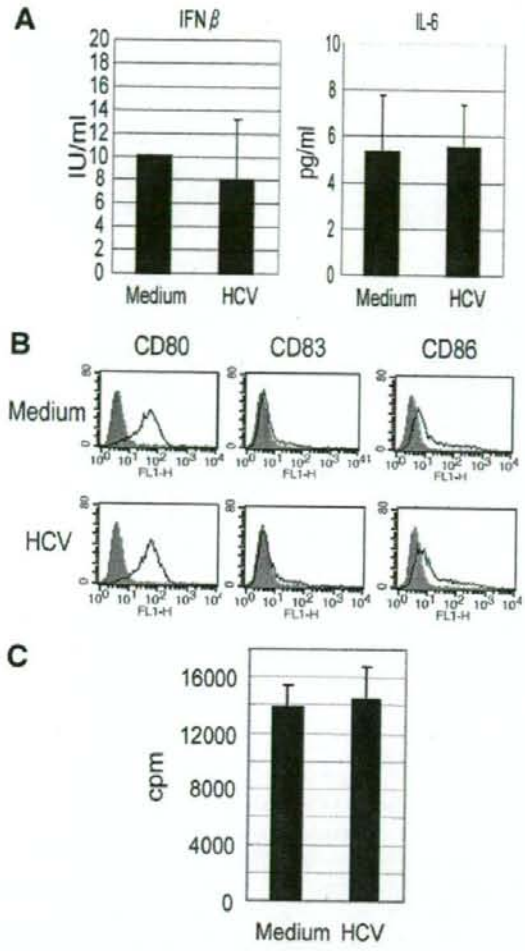

Fig. 2. HCV fails to induce MoDC maturation and cytokine response. MoDCs were inoculated with HCV at an MOI of 1 and cultured for 48 hours. (A) The supernatant was assayed for production of IFN-beta and IL-6. (B) The cells were harvested for FACS and (C) mixed lymphocyte reaction (MIR). Allogeneic PBMC were cultured with the inoculated-MoDCs for 6 days. Proliferation was determined by [^{3}H]thymidine uptake. Data show means ± SD of duplicate or triplicate samples from one experiment representative of three donors.

treated with mitomycin C and cultured with allogeneic $CD4^+$ T cells (1×10^5) for 6 days. Then the cells were washed and transferred to new round-bottom 96-well plates. Phorbol 12-myristate 13-acetate (10 ng/mL; Sigma-Aldrich) and ionomycin (1 μg/mL; Sigma-Aldrich) were added and plates were incubated for a further 24 hours. Supernatants were harvested for cytokine production (IL-4, IFN-gamma; GE-Healthcare).

MoDC-NK Coculture and ^{51}Cr Release Assay. The stimulated-MoDCs were harvested for MoDC-NK coculture at indicated time points. Autologous NK cells (5×10^5) were cocultured with the MoDCs (1×10^5) in 24-well plates for 24 hours. Transwell (Corning) was inserted to block the MoDC-NK cell contact. The supernatants and NK cells were collected from the MoDC-NK coculture and assayed for IFN-gamma production (GE Healthcare) and cytotoxicity against K562. Cytotoxicity was determined by standard ^{51}Cr release assay as described.[17]

Gene Silencing of TLR3 in MoDC. Small interfering RNA (siRNA)-based gene knockdown was preformed with MoDCs by electroporation as described.[21] siRNA duplexes (small interfering TLR3: cat #107056, negative control: cat #AM4635) were obtained from Ambion (Tokyo, Japan). Expression of TLR3 was examined by SYBR green real-time PCR using forward primer, AAGACCCATTATG-CAAAAGATTCAA and reverse primer, TCCAGATTTT-GTTCAATAGCTTGTTG. MoDCs (1×10^6 cells) were electroporated with these siRNA and cultured for 4 hours. Then, HCV-infected or noninfected apoptotic Huh7.5.1

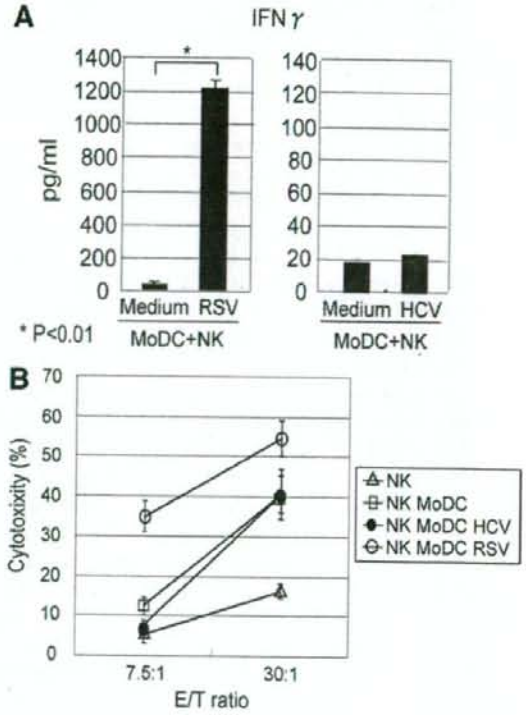

Fig. 3. MoDCs inoculated with HCV barely activate NK cells. MoDCs were harvested at 24 hours after inoculation of RSV and HCV. Autologous NK cells were cocultured with the MoDCs for 24 hours. (A) The supernatant were assayed for NK IFN-gamma production. (B) NK cells were harvested for ^{51}Cr release assay to examine NK cytotoxic activity against K562. A representative of the three similar experiments with individual donors is shown.

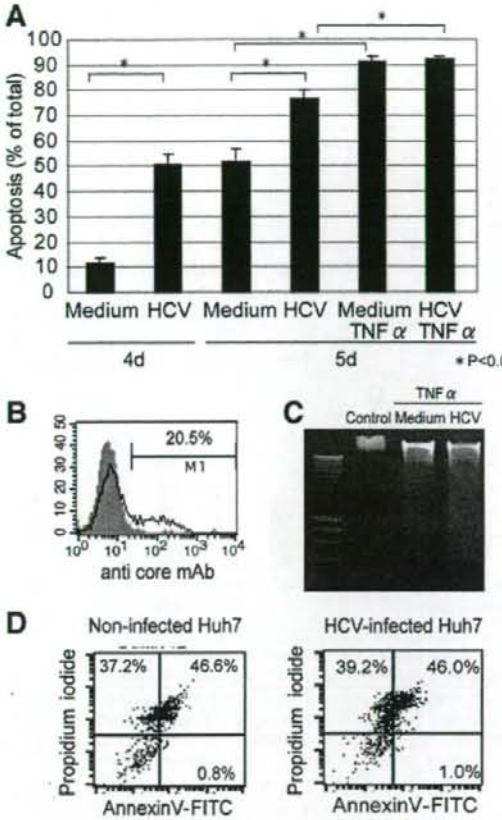

Fig. 4. Preparation of HCV-infected apoptotic Huh7.5.1 cells. Huh7.5.1 cells were infected with HCV at an MOI of 1 and culture for 4 or 5 days. Apoptosis was induced by cycloheximide and TNF-alpha after 4 days culture. At 5 days after infection, the apoptotic cells were harvested for counting 4′,6-diamidino-2-phenylindole stained apoptotic nuclei, FACS and examination of DNA fragmentation. (A) Typical apoptotic cells stained with 4′,6-diamidino-2-phenylindole were counted among <1000 cells and percent cell apoptosis was determined. Data are means ± SD from three independent experiments, each performed in triplicate. (B) HCV-core antigens were detected in the HCV-infected apoptotic cells by FACS. (C) DNA was extracted from HCV- or noninfected apoptotic Huh7.5.1 cells and electrophoresed on agarose gels to evaluate DNA fragmentation. (D) HCV- and noninfected Huh7.5.1 cells were examined for stages of apoptosis by FACS using annexin V-fluorescein isothiocyanate (FITC) and proidium iodide. Data shown are representative of three independent experiments.

cells (2×10^6 cells) were added to the wells. After 48 hours of culture, the supernatants were harvested and examined for cytokine concentrations by ELISA.

Results

MoDCs Are Not Permissive for HCV Replication. MoDCs and Huh7.5.1 cells were inoculated with the JFH1 strain at an MOI of 1, then the cells were harvested for immunofluorescent staining and sequence-specific real-time RT-PCR at indicated time points after inoculation. HCV genome RNA (negative sense of HCV RNA) was replicated in Huh7.5.1 cells but not to a detectable level in MoDCs at 2 to 3 days after inoculation (Fig. 1B). Accordingly, HCV core antigens were detected in Huh7.5.1 cells, but not in MoDCs, by immunofluorescent staining until 3 days after HCV inoculation (Fig. 1A). Similar results were obtained with monocyte-derived macrophages and BDCA4$^+$ pDCs (data not shown).

MoDC Maturation and Cytokine Response Against the JFH1 Strain. DCs work as key producers of innate inflammatory cytokines in response to pathogen-associated molecular patterns (PAMPs). However, MoDCs inoculated with JFH1 (MOI = 1) did not produce IFN-gamma or IL-6 over the noninfected control (Fig. 2A). MoDCs stimulated with PAMPs mature to up-regulate CD80/CD86 expression and activate T cells. Some reports showed that the MoDC maturation was induced following incorporation of HCV pseudotype particles into the MoDCs.[22] However, expression of costimulatory molecules (CD80, CD86) and a maturation marker (CD83) were not up-regulated by inoculation with the JFH1 strain (MOI = 1; Fig. 2B). MoDCs cocultured with JFH1 strain did not enhance the proliferation of allogeneic PBMC compared with noninoculated MoDCs (Fig. 2C).

MoDCs Exposed to the JFH1 Strain Do Not Activate NK Cells. MoDCs are known to recognize PAMPs and promote NK cell activation via MoDC/NK reciprocal interaction.[9] We have reported that NK cells are activated by MoDCs infected with RNA viruses, such as RSV, influenza virus, and measles virus.[17] We inoculated MoDCs with RSV or the JFH1 strain at an MOI of 1 and cocultured the MoDCs with autologous NK cells. After 1-day of coculture, NK cell IFN-gamma and cytotoxicity were markedly induced by RSV-treated MoDCs but not HCV-treated MoDCs (Fig. 3A,B).

HCV-Infected Apoptotic Cells Induce MoDC Maturation and Cytokine Responses. Then, we moved on to whether HCV-infected cells affect MoDC maturation. We first cocultured MoDCs with HCV-infected or noninfected Huh7.5.1 cells and examined IL-6 production by MoDCs. MoDCs cocultured with HCV-infected Huh7.5.1 cells secreted more IL-6 than those with noninfected Huh7 cells (Fig. 5A). However, since HCV infection induced apoptosis in Huh7.5.1 cells, HCV-infected and noninfected Huh7 cells were not in the same apoptotic stages (Fig. 4A). We had to exclude the possibility that apoptotic events themselves affect MoDC maturation. Therefore, we forced HCV-infected and

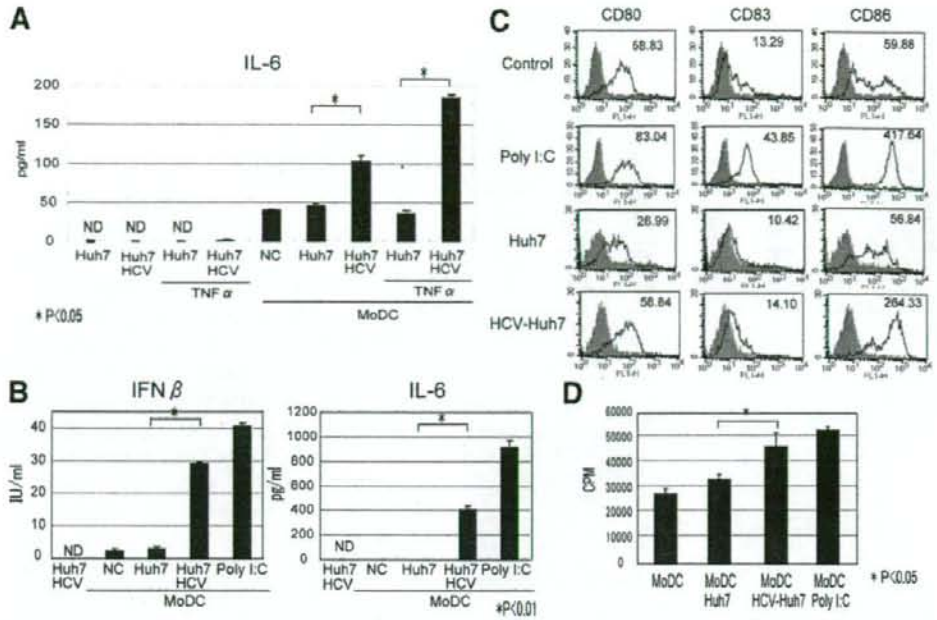

Fig. 5. HCV-infected apoptotic cells induce MoDC maturation and cytokine response. MoDCs were cocultured with HCV-infected/noninfected apoptotic or nonapoptotic cells for 2 days. Polyl:C stimulation was used as a positive control. (A,B) The culture supernatants were assayed for determination of IFN-beta and IL-6. The MoDCs were isolated from the apoptotic cells and used for (C) FACS and (D) mixed lymphocyte reaction (MLR). MoDC maturation was examined by the expression of CD80, CD83, and CD86 (C, a representative of three donor experiments). Allogeneic PBMCs were cultured with the MoDCs for 6 days. Proliferation was determined by [^{3}H]thymidine uptake (D, means ± SD of triplicate samples from one representative of three donors).

noninfected cells to induce full apoptosis by cycloheximide and TNF-alpha to the same level of apoptotic stages (Fig. 4A). HCV core antigens were detected in 20.5% of the HCV-infected apoptotic cells (Fig. 4B). Apoptotic nuclei were observed in almost all of HCV-infected and noninfected cells (Fig. 4A). DNA ladder formation, a hallmark of apoptosis, was detected in HCV-infected and noninfected apoptotic Huh7.5.1 cells to similar levels (Fig. 4C). Apoptotic cells, either infected or noninfected, gave similar profiles by flow cytometry using annexin-V for early apoptosis and propidium iodide for late apoptosis (Fig. 4D).

We applied these HCV-infected and noninfected apoptotic cells to MoDCs and determined the concentration of IFN-beta and IL-6 in the culture supernatants. HCV-infected apoptotic cells facilitated the production of IFN-beta and IL-6 by MoDCs compared with noninfected apoptotic cells (Fig. 5B). In this context, HCV products, rather than undergoing apoptosis, in infected cells are an essential factor for induction of MoDC maturation (Fig. 5A).

We next examined whether MoDC maturation was induced by HCV-infected apoptotic cells. After coculture of MoDCs with the apoptotic cells, MoDCs were isolated from the apoptotic cells using Ficol Paque. Purity of these isolated MoDCs reached over 98%, judged by 5(6)-Carboxyfluorescein diacetate N-succinimidyl ester labeled MoDCs (data not shown). CD86 of the maturation markers on MoDCs (Fig. 5C) was especially more expressed on these cells by HCV-infected apoptotic cells than by noninfected apoptotic cells. HCV-infected apoptotic cells slightly enhanced the expression levels of major histocompatibility complex class I, class II, and human leukocyte antigen-E on MoDCs (data not shown). MoDCs also acquired the increased ability to stimulate allogeneic PBMCs, $CD4^+$ T cells, and $CD8^+$ T cells in response to HCV-infected apoptotic cells (Figs. 5D and 6A).

We determined the ability of $CD4^+$ T cells to produce IFN-gamma (a Th1 cytokine) and IL-4 (a T helper 2 cytokine) after coculture of allogeneic $CD4^+$ T cells and MoDCs exposed to HCV-infected apoptotic cells. These $CD4^+$ T cells produced higher levels of IFN-gamma and lower levels of IL-4 (Fig. 6B) compared to the noninfected control, suggesting that HCV-infected apoptotic cells modulate MoDC func-

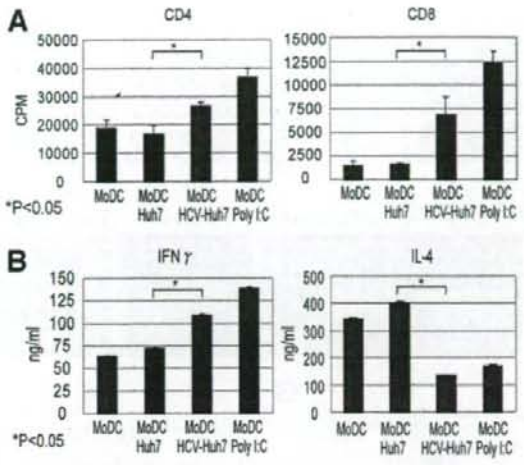

Fig. 6. HCV-infected apoptotic cells modulate MoDC function to polarize the Th1 shift. (A) After 2 days culture with HCV-infected and noninfected apoptotic cells, the isolated MoDCs (1×10^4) were cultured with allogeneic CD4+T cells and CD8+ T cells (1×10^5) for 6 days. Proliferation was determined by [^{3}H]thymidine uptake. (B) Allogeneic CD4+ T cells were harvested after 6 days culture with the MoDCs and stimulated with phorbol 12-myristate 13-acetate and ionomycin for 24 hours. The supernatants were collected to assess the levels of IFN-gamma and IL-4 by ELISA. Poly I:C stimulation was used as a positive control. Data shown are means ± SD of duplicate or triplicate samples from one experiment representative of three donors.

tion to promote Th1-dominant immunity in the Th1/T helper 2 balance.

HCV-Infected Apoptotic Cells Stimulate MoDCs To Activate NK Cells. We next evaluated whether these mature MoDCs could enhance NK activity via MoDC-NK interaction. After exposure of MoDCs to HCV-infected or noninfected apoptotic cells, MoDCs were isolated as described above. HCV-infected apoptotic cells promoted MoDC function to augment NK cell cytotoxicity but not IFN-gamma production compared to noninfected cells (Fig. 7A,B). This up-regulation of NK cell cytotoxicity through MoDC-NK interaction was canceled by separating MoDCs from NK cells with a transwell insertion (Fig. 7C). This suggested that cell-cell contact was the key factor for MoDC-mediated NK cell cytotoxicity induced by coculture with HCV-infected apoptotic cells.

MoDC Maturation Relied on TLR3 Signal Evoked by dsRNA in Apoptotic Vesicles. We surveyed the mechanism of MoDC maturation by HCV-infected apoptotic cells. Since HCV is a positive single-strand RNA virus, dsRNA was detected in HCV-containing apoptotic vesicles by mAb against dsRNA (Fig. 8A). To investigate whether MoDCs were taking up these apoptotic vesicles, we labeled HCV-infected apoptotic cells with the far red fluorescent dye, SNARF-1. MoDCs phagocytosed the SNARF-1-labeled vesicles containing dsRNA, which partially colocalized with TLR3 (Fig. 8B,C). N-[1-(2,3-Dioleoyloxy)propyl]-N, N, N-trimethylammonium methylsulfate (DOTAP)-based transfection was employed for the targeting of RNA to the TLR3-containing endosome.[23] HCV-derived RNA allowed MoDCs to induce IL-6 production as in control poly I:C (Fig. 8D). IL-6 of

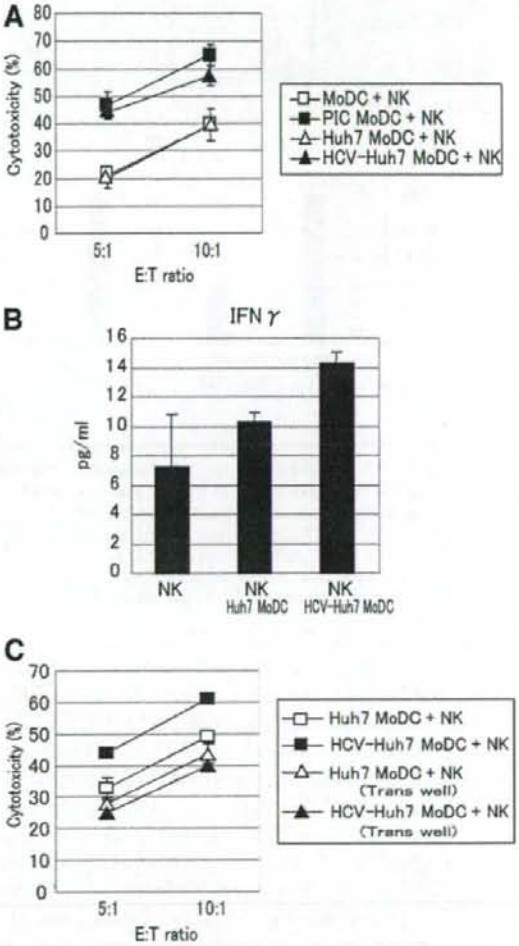

Fig. 7. NK cell activation by MoDCs exposed to HCV-infected apoptotic cells. After 2 days culture with HCV-infected and noninfected apoptotic cells, the isolated MoDCs were cultured with autologous NK cells for 24 hours. (A) NK cytotoxic activity against K562 was determined by ^{51}Cr release assay. Poly I:C stimulation was used as positive control. (B) Supernatant of the MoDC-NK coculture was assayed for NK cell IFN-gamma production. In some experiments, transwell was used to block MoDC-NK cell contact. (C) Using these NK cells, cytotoxic activity was measured by ^{51}Cr release assay. Data shown are means ± SD of duplicate or triplicate samples from one experiment representative of three donors.